RPSEA

Final Report
Small Producers Program

Development Strategies for Maximizing
East Texas Oil Field Production

Contract No. 08123-16

July 15, 2014

Fred P. Wang
Research Scientist
Bureau of Economic Geology, Jackson School of Geosciences
10100 Burnet Rd., Bldg. #130, Austin, TX 78750

LEGAL NOTICE

This report was prepared by the Bureau of Economic Geology, The University of Texas at Austin, as an account of work sponsored by the Research Partnership to Secure Energy for America, RPSEA. Neither RPSEA, members of RPSEA, the National Energy Technology Laboratory, the U.S. Department of Energy, nor any person acting on behalf of any of the entities:

a. MAKES ANY WARRANTY OR REPRESENTATION, EXPRESS OR IMPLIED, WITH RESPECT TO ACCURACY, COMPLETENESS, OR USEFULNESS OF THE INFORMATION CONTAINED IN THIS DOCUMENT, OR THAT THE USE OF ANY INFORMATION, APPARATUS, METHOD, OR PROCESS DISCLOSED IN THIS DOCUMENT MAY NOT INFRINGE PRIVATELY OWNED RIGHTS, OR

b. ASSUMES ANY LIABILITY WITH RESPECT TO THE USE OF, OR FOR ANY AND ALL DAMAGES RESULTING FROM THE USE OF, ANY INFORMATION, APPARATUS, METHOD, OR PROCESS DISCLOSED IN THIS DOCUMENT.

THIS IS A FINAL REPORT. THE DATA, CALCULATIONS, INFORMATION, CONCLUSIONS, AND/OR RECOMMENDATIONS REPORTED HEREIN ARE THE PROPERTY OF THE U.S. DEPARTMENT OF ENERGY. REFERENCE TO TRADE NAMES OR SPECIFIC COMMERCIAL PRODUCTS, COMMODITIES, OR SERVICES IN THIS REPORT DOES NOT REPRESENT OR CONSTITUTE AN ENDORSEMENT, RECOMMENDATION, OR FAVORING BY RPSEA OR ITS CONTRACTORS OF THE SPECIFIC COMMERCIAL PRODUCT, COMMODITY, OR SERVICE.

THIS PAGE INTENTIONALLY LEFT BLANK

ABSTRACT

The goals of this project were to evaluate deepening and behind-pipe opportunities and enhanced oil recovery (EOR) potentials to maximize recovery from the East Texas Oil Field (ETOF), a giant mature and marginal field currently operated by 114 small producers. This field-demonstration project has two industrial partners, Danmark Energy LLP and John Linder Operating Co., and two primary goals: (1) locating well-deepening and waterflooding targets guided by depositional trends through detailed mapping of reservoir architecture, and (2) conducting a feasibility study on EOR methods for recovering a portion of the ~1.1 billion stock tank barrels (BSTB) of residual oil. The processes are low cost, low risk, and potentially highly profitable. While the geographic scope of the project was limited to only parts of the giant ETOF, results should serve as an important geologic and engineering research source to provide crucially needed support to all operators in the field. Research findings have already been efficiently transferred into production enhancement for many operators.

Depositional environments of lower stringer sandstones in the northern and middle parts of the ETOF were mapped using >600 wells, and deepening candidates were identified based on architecture of depositional systems. With the help of results from this study, 8 out of 15 workover/recompletion targets successfully produced more than 140,000 STB of crude at a low cost about $1 million. With net revenues of ~ $11 million on these deepenings and workovers alone, the project has already created considerable benefits for operators.

Both surfactant/polymer and CO_2 floodings were tested in the laboratory using ETOF and Berea sandstone cores. Oil recovery of 70% by miscible CO_2 flooding in ETOF cores is slightly lower than 85% recovery in Berea sandstone cores. Oil recovery by alkaline-surfactant-polymer (ASP) flooding in Berea and ETOF cores is 90% and 28%, respectively. Significantly lower oil recovery in ETOF cores might have stemmed from the high adsorption of surfactant by clay minerals; in addition, the optimal three-phase condition was not achieved in the core flooding.

TABLE OF CONTENTS

EXECUTIVE SUMMARY

The East Texas Oil Field (ETOF), the second most productive oil field in the United States based on cumulative production, has produced 5.43 billion stock tank barrels (BSTB) from lower Woodbine sandstones since 1930. It has been one of the best-performing giant fields in the world, but it is now an aging giant, operated by a large number of small producers who encounter enormous technical, economic, and environmental challenges. Currently, 114 out of 117 operators in the field are small producers.

The objectives of this 3-year study are to explore short- and midterm strategies for maximizing recovery from the ETOF. After 84 years of production, more than 1.5 billion barrels (Bbbl) of oil remain in the reservoir and are exceedingly difficult to recover. Development of strategies to recover this oil has become critical because operators, who as explained above are mostly small producers, do not have sufficient expertise or support in geology or engineering, which are crucial to revitalizing production as well as to lowering production cost.

Currently ~1,580 million stock tank barrels (MMSTB) of oil remains in the reservoir—480 MMSTB of this total is remaining mobile oil and 1,100 MMSTB is residual oil. Of the 480 MMSTB of remaining mobile oil, ~70 MMSTB (Wang and others, 2008) will be produced by 2030 using current practices, according to decline-curve analysis; and 410 MMSTB is untapped, unswept, or poorly swept. A fraction of the 400 MMSTB of remaining mobile oil can be produced using strategically targeted recompletions and waterfloods guided by depositional trends, whereas residual oil can be produced only by enhanced oil recovery (EOR) methods.

In spite of the field's excellent reservoir quality and stunning long-term performance history, details of its depositional environment and reservoir architecture have not been fully studied and have only recently become better understood (Ambrose and Hentz, 2010). This project comprises (1) a short-term field-demonstration project on depositional-trend–guided deepenings and waterfloods; and (2) a midterm research project on long-term recovery strategies, including feasibility studies of (a) CO_2 flooding, (b) surfactant/polymer flooding, and (c) their economic and environmental impacts.

The project area covered about two-thirds of the ETOF, >80 mi^2 and containing 10,000 wells. Goals of the short-term demonstration project are (1) to demonstrate the technology of strategically targeted deepenings and optimized waterfloods guided by depositional trends, and (2) to identify deepening targets and waterflood sites, which has the potential to increase the

short-term oil production from untapped, unswept, or poorly swept remaining mobile oil in the ETOF project area.Results of these field tests will allow us to estimate reliably the recoverable fraction of the 410 MMSTB remaining mobile oil, and results of laboratory EOR tests will provide us crucial information about the recovery factors of 1.1 BSTB residual oil. Technical, economic, and environmental impacts of EOR methods on ETOF are evaluated. The resulting GIS database with well locations, raster logs, production data, and depositional-trend maps will be made available to all operators in the field.

As a field operated by a large number of small producers, the ETOF perfectly illustrates the situations and dilemmas faced by numerous other mature and marginal fields in the United States. This large, semi-fieldwide study develops techniques and methods of increasing short-term oil production, as well as maximizing long-term oil recovery for all small producers in the ETOF. These techniques are low cost, low risk, and potentially highly profitable, even at lower oil prices. The techniques can also be applied to other similarly mature and marginal fields in the United States that are operated by small producers.

INTRODUCTION

The East Texas Oil Field (ETOF), discovered on September 3, 1930, has produced 5.44 billion stock tank barrels (BSTB) of 39^{o} American Petroleum Institute (API) oil from lower Woodbine sandstones in >31,000 wells. Estimated original oil in place (OOIP) varies from 6.8 to 7.5 BSTB in table 1 (Gussow, 1973; Galloway and others, 1983; East Texas Engineering Association, 1953; Casey Engineering Inc., 1994; Wang, 2010). Given a midrange OOIP value of 7.0 BTSB, current recovery efficiency is 77%, which is the highest of any giant oil field in the world.

After 84 years of production, >1.5 billion barrels (Bbbl) of oil remains in the reservoir. Targeting and producing this oil has proven difficult. Since the late 1990's, major oil companies have sold most of their properties to small producers. Development of strategies to recover this oil has become a critical issue because most current operators do not have sufficient expertise and support in geology and engineering, which are crucial to revitalizing production as well as to lowering production cost.

In spite of the field's excellent reservoir quality and remarkable long-term performance history, details of its depositional environment and reservoir architecture have not been fully studied and have only recently become better understood (Ambrose and Hentz, 2010). Currently, ~1,570 million stock tank barrels (MMSTB) of oil remains in the reservoir—470 MMSTB of this total is remaining mobile oil and 1,100 MMSTB is residual oil. Of the 470 MMSTB of remaining mobile oil, ~70 MMSTB (Wang and others, 2008) will be produced by 2030, according to decline-curve analysis; and 400 MMSTB is untapped, unswept, or poorly swept. A fraction of the 400 MMSTB remaining mobile oil can be produced using strategically targeted recompletions and waterfloods guided by depositional trends, whereas residual oil can be produced only by enhanced oil recovery (EOR) methods.

FIELD HISTORY AND PRODUCTION

The ETOF (fig. 1) is located on the west flank of the Sabine Uplift in Gregg, Rusk, Upshur, Smith, and Cherokee Counties adjacent to the East Texas Basin. With 7.0 BSTB of estimated original oil in place, it is the second-largest field in the United States after Prudhoe Bay Oil Field in Alaska. The ETOF is not only a successful oil field but also the birthplace of many production technologies and theories. Its success set forth the exploration strategy of "looking for updip stratigraphic traps" (Levorsen, 1934), which led to several large discoveries, including that of the giant Prudhoe Bay field in Alaska (Anonymous, 2003). With the exception of the field's early chaotic development history and overproduction, through the efforts of government and major operators, the ETOF has been a well-regulated and well-managed field. The Woodbine sandstone in the ETOF is a wedge-type reservoir at subsea depths of between –3,100 and –3,300 ft, with pay thicknesses of as much as 120 ft (fig. 2). It is bounded by the subregional, pre–Austin Chalk unconformity (Minor and Hanna, 1933) at the top and the Buda Limestone or the regional aquifer at the base. The Woodbine reservoir in the ETOF is composed of predominantly nonmarine sandstones and conglomerates (Minor and Hanna, 1933) in the main Woodbine and deltaic sandstones (Ambrose and others, 2010) in the lower part of the Woodbine.

The Woodbine main pay fluvial-channel sandstone in the north (figs. 7, 8) is commonly massive and homogeneous, with average porosity and permeability of 25% and more than 2,000 md (table 2). This main sandstone is well connected to the downdip aquifer. The underlying lower-quality deltaic sandstones are thin and highly heterogeneous (Ambrose and others, 2010). These highly compartmentalized deltaic sandstones below the main Woodbine channel sandstone are normally not connected to the downdip aquifer.

The early history of the ETOF is one of rapid development, with 3,612 and 9,372 wells completed by the end of 1931 and 1932, respectively. The number of producing wells reached 25,829 in 1939. With 30,580 wells, the ETOF is one of the most densely drilled fields in the world, with an average well spacing of 4.2 acres (ranging from 0.05 to 15 acres).

The current daily production rate is ~10,084 barrels of oil per day (bbl/d) from 3,886 wells. Yearly production (green curve in fig. 3c) peaked at 207 MMSTB in 1933, declined to 40 MMSTB in 1964, increased again to 77 MMSTB in 1972, and then declined to 8.7 MMSTB in 2000, when the water cut exceeded 99%. Production further gradually declined to 4.5 MMSTB in 2012. The initial period of decline from 1933 to 1964 was caused by a decrease in reservoir

pressure, number of producing wells, and number of monthly production days (fig. 3). The second increase in production from 1965 to 1972 resulted from an increase in the number of monthly production days allowed by the Texas Railroad Commission from 8 to 26.

The East Texas Engineering Association (1953) assessed OOIP at 6.84 BSTB and estimated ultimate recovery (EUR) at 5.42 BSTB (79%). The 1994 study by Casey Engineering, Inc., assessed OOIP and EUR at 7.03 and 5.64 BSTB, respectively (recovery efficiency of 80%). The high recovery efficiency of the field has been attributed to (1) high reservoir quality and continuity; (2) favorable wedge geometry, thickness, and stratigraphic dip; (3) effective water drive; (4) good crude quality; (5) low residual oil saturation; (6) high sweep efficiency; and (7) successful production management, including conservation, plugback, downdip water injection, well deepening, waterflooding, and miniwaterflooding. Most of these aspects apply to the main Woodbine sandstone interval but not to the underlying stringer sandstones.

Major technologies used in the field are **(1) downdip water injection, (2) plugback, (3) deepening, (4) waterflooding, (5) polymer flooding,** and **(6) miniwaterflooding**.

Downdip Water Injection

Downdip water injection started in 1938 and is conducted primarily to dispose of produced water and, to some extent, maintain reservoir pressure. Because Woodbine main pay fluvial-channel sandstones in the north are commonly massive and homogeneous, water is normally produced from the bottom of the sandstone interval, keeping oil production from the upper interval. In addition, two-thirds of the wells penetrated only part of the upper interval to avoid excessive amounts of produced water.

Plugback

Because of the very strong bottom-water drive, as oil production proceeded in the ETOF, the oil–water contact rose within the main-pay reservoir interval. To prevent wells from producing excessive amounts of water, plugback operations were undertaken and were very successful in reducing water production (Minor and Hanna, 1941; East Texas Engineering Association, 1953). Because of the good reservoir quality of the main-pay interval, as water encroached from the base, effective recompletions were made at higher levels within the main-pay sand.

Deepening

The shallow wells in the ETOF missed some significant compartmentalized deep targets, so starting in the late 1930's and continuing to the present, well deepening has been one of the primary strategies for recovering untapped oil. Deepening of existing wells is done primarily to exploit laterally discontinuous "stringer" sandstones in the deltaic succession that are inferred to compose limited, untapped reservoir compartments because of abrupt lateral and vertical changes in thickness of sandstone bodies. Figure 4 shows an early deepening example. The well was initially drilled to –3,281 ft, with a thick channel sandstone at the top and thin stringer sandstones at the base. When the well watered out in 1947, it was deepened to –3,335 ft, and two more stringer sandstones with favorable resistivities were found at the interval between –3,281 and –3,309 ft. The well was perforated from –3301 to –3309 ft and produced 497 bbl/d in 1947; as of November 5, 1951, it had produced 37,509 STB.

More than 2,600 wells have been deepened, with a maximum of 114 completed in 1975 (Fig. 3b). Most deepenings occurred between 1956 and 1998. Several recent deepenings produced >55 bbl/d with zero to little water (Nault, Danmark Energy, oral commun., 2008). Although deepening is still one of the current practices in the ETOF, the number has decreased to fewer than 5 per year since 1999, after major oil companies sold most of their properties to small producers. Deepening targets have become exceedingly difficult for small producers to find because they do not have sufficient technical support.

Depositional trends of lower stringer sandstones were mapped by the Bureau of Economic Geology (BEG) from 2006 to 2010 (Ambrose and others, 2010) through pilot studies of the Castleberry Survey in the north, the South Kilgore Unit in the middle, and the ARCO waterflooding area in the south (Pena-Cadena Survey). Different from the Woodbine main pay fluvial channel, the lower stringers were deposited in a deltaic setting, as detailed in the Sequence Stratigraphy section of this report.

Waterflooding

Because of the change in depositional environment, the reservoir quality of Woodbine sandstone decreases from north to south. Moreover, the updip reservoir in the middle to south parts of the ETOF did not get sufficient pressure support from the downdip aquifer. Waterfloods have been implemented in the central and south parts of the field in areas with poorer and more discontinous reservoir quality compared to the main pay. Examples include the Daisy Bradford area, the updip of the Pena-Cadena Survey (South Pilot area), and the South Kilgore Unit.

These waterfloodings have increased the reservoir pressure and improved oil recovery. The South Kilgore Unit and the South Pilot area are two of the best producing areas in the ETOF in the last 10 years.

Polymer Flooding

Polymer flooding, which does not lower residual oil saturation, is normally used to enhance oil recovery by improving the vertical sweep efficiency of waterflooding operations through mobility control, the viscous polymer solution diverting more water into tighter intervals. Polymer floodings were tested by industrial operators in three areas: the Hunt Pilot–Daisy Bradford area in 1982, the W. H. Siler Lease in 1984, and the I. L. Kinney #70 area in 1985. The floodings were successful to a limited degree because the mobility ratio between the ETOF oil and brine is relatively low and polymer flooding works better for reservoirs with a higher mobility ratio.

Miniwaterflooding

Recently, miniwaterfloods have also been used to improve recovery from poorly connected lower stringer sandstones (Nault, Danmark Energy, oral commun., 2008). This process can increase production three- to fivefold in normal wells, and by as much as twentyfold in good wells. Miniwaterfloods work better in areas where lower stringer sandstones are relatively thick and locally connected, with multiple well penetrations. Operator understanding of geological connectivity of stringer sandstones is presently very limited.

With EUR of 5.64 BSTB and cumulative production of 5.44 BSTB as of October 31, 2013, 400 MMSTB of mobile oil still remained in the ETOF (fig. 5). According to decline-curve analysis, only 70 of the 400 MMSTB of remaining mobile oil will be produced by 2030 under current operations practices (Wang and others, 2008). Of the recoverable remaining mobile oil, ~330 MMSTB will remain untapped and unswept.

Part of the untapped and unswept mobile oil can be produced by deepening/recompletion and optimizing water injection locations, but residual oil can only be produced by enhanced oil recovery methods. Two types of untapped oil in the ETOF are (1) oil in the lower stringer sandstones below the main Woodbine and below the original oil–water contact, and (2) oil at the low-quality sandstone above the main Woodbine sandstone.

Deepening/recompletion is a low-cost and low-risk operation that could slow down production decline (fig. 6). Since 1999, oil from the ETOF has been produced predominantly by downdip water injection and by scattered deepenings and miniwaterfloods. Since water flooded the entire main-pay Woodbine sandstone around the year 2000, average well production has declined to ~3 bbl/d, with a 99% water cut. Most expenses are associated with disposing of the produced water. Deepenings target the lower Woodbine deltaic stringer sandstones. These sands are poorly connected to the downdip aquifer and can produce oil with zero to little water. The operating costs of these deepening wells are much less than those of most wells that produced from the main Woodbine sandstone because high-volume water handling is not required. The lack of geologic and engineering support to the 110 small producers in the field has made finding these targets technically difficult and economically risky, however.

Strategically targeted deepenings and waterfloods—small or large, guided by depositional trends—are low cost, low risk, and potentially highly profitable, as well as being the most economically viable technologies for enhanced ETOF short-term production. The BEG pilot studies clearly demonstrated the viability of expert mapping of depositional trends to reduce risks in finding deep lower-stringer sandstones. This study extends the BEG pilot studies to a geographically larger area of mapped depositional trends and reservoir architecture as a guide for locating workover, deepening, and waterflooding targets.

EOR methods are needed to recover the ~1.1 BSTB of remaining oil in the ETOF. Except for several polymer injection pilots, no other EOR methods have been tested in the laboratory or field. A preliminary screening study by Wang and others (2008) suggests that the ETOF will face many technical, economic, and environmental challenges in applying EOR methods. Another objective here is to study the feasibility of various EOR methods for the ETOF.

METHODOLOGY

The project is an integrated geologic and engineering characterization of two-thirds of the ETOF—approximately 150 mi^2 and more than 10,000 wells. It is divided into three phases (each of 1-year duration) (fig. 1) and comprises five overall components:

- Phase I area study
- Phase II area study
- Phase III area study
- Field tests
- EOR laboratory tests and feasibility study

Procedures

1. Data Compilation and Database Implementation

Approximately 5,000 wireline logs were collected from the East Texas Engineering Association (ETEA) library and individual operators. They were scanned and loaded into databases for geologic and engineering study. These databases were accessed with PETRA software and used mainly for geologic correlation and mapping.

2. Geologic Characterization

2.1 Well-tops determination and net sandstone calculation

The top of the main Woodbine sandstone was picked in all wireline logs usedin this study. The top of Buda was identified in deep wells, and the base of the main Woodbine sandstone was picked as the upper boundary of lower stringers.

2.2 Well correlation and depositional-trend mapping

Stratigraphic units were correlated using cross sections to determine reservoir architectures. Woodbine sandstone and Buda formations were correlated using deeper wells penetrating the Buda formation. The main Woodbine sandstone and the lower-stringer sandstone were correlated using wells with intermediate depths. The lower stringer was further divided into 3-to-5 subunits through geologic correlation.

2.3 Cutoff criteria for lower-stringer pay

We used gamma-ray (GR) and spontaneous-potential (SP) curves to determine the net sandstone thickness and resistivity to estimate the thickness of pay. A set of cutoff values in resistivity was used to determine whether the interval is pay or not.

2.4 Calculation of net sandstone thickness of each unit

Net sandstone thickness of each unit was calculated using SP and GR cutoff values for each subunit of the stringer sandstone.

2.5 Structure and net sandstone thickness maps to determine depositional trends

Structure and thickness maps were prepared using the interval tops determined in 2.2.

3. Petrophysical Properties and Engineering Analysis

3.1 Characterization of petrophysical properties using core and wireline log data

Porosity, permeability, connate water saturation, and residual oil saturation were determined from core data and wireline logs.

3.2 Analysis of well-completion and production history

Well-completion and production data were analyzed to identify where oil and water have been produced from and behind pipe potentials.

4. Workover Target Identification and Ranking

4.1 Identification of potential targets for deepening and waterflood using depositional-trend maps

After the 1st-year study, targets for deepening and recompletion, as well as for miniwaterflood, were identified with our partners Danmark Energy LP and Linder Operating Co., using depositional-trend maps.

4.2 Elimination of shut-in, depleted and problematic, and commingled locations

Before identifying deepening and recompletion targets, we eliminated shut-in, depleted and problematic, and commingled locations.

4.3 Estimation of oil reserve of each location

The reserve of each location was estimated using net sandstone thickness and the shape of GR or SP curves.

4.4 Ranking of potential targets

Selected targets were ranked according to their production potentials.

5. Miniwaterflood Design and Field Test

5.1 Selection of potential waterflood sites

Sites for miniwaterflooding were identified based on maps of reservoir architectures and well distribution in the lease and adjacent leases, and ranked by volumes of untapped stringer sandstones.

5.2 Design of waterflood patterns based on depositional-trend maps and active well locations

Opportunities for waterfloods were not pursued because industry partners decided against the investments, preferring to expand their deepening programs.

6. Laboratory EOR Tests

6.1 Selection of cores for EOR tests

Core plugs were cut from the ETOF core in BEG, and porosity and permeability of each plug measured.

6.2 Measurement of CO_2 minimum miscibility pressure with ETOF crude

Slim-tube tests were conducted to determine CO_2 minimum miscibility pressure with ETOF crude.

6.3 Laboratory tests on miscible and immiscible CO_2 floodings

A series of laboratory tests were performed on Brea and ETOF cores to determine recovery efficiencies of miscible and immiscible CO_2 floodings.

6.4 Phase behavior of surfactant/polymer systems

We studied phase behaviors among ETOF crude/surfactant–cosolvent/brine systems, including effects of salinity and of surfactant type and concentration. Compositions of ETOF crude/surfactant–cosolvent/brine systems will be tested to find optimal conditions.

6.5 Laboratory tests of surfactant/polymer flooding

A series of laboratory tests will be performed on Brea and ETOF cores to determine recovery efficiencies of selected surfactant/polymer systems.

6.6 Economic and environmental impacts of EOR

If laboratory tests were favorable, then economic and environmental considerations would have been pursued in detail.

DISCUSSION

Sequence Stratigraphy

The Woodbine Group was deposited during a major middle- and late-Cenomanian regressive event following a pronounced lowering of relative sea level after the Buda and before the Woodbine deposition, which affected the entire Gulf Coast Basin (Salvador, 1991; Mancini and Puckett, 2005). A maximum of 14 fourth-order sequences occur within the greater Woodbine succession (top of Buda Limestone to lowermost Eagle Ford Group) in the central part of the East Texas Basin, where the unit is complete (Ambrose and others, 2009; Hentz and Bonnaffé, 2010). Sequence boundaries (SB), transgressive surfaces of erosion (TS), and maximum flooding surfaces (MFS) within the sequences were inferred primarily from the logs' gamma-ray signatures, supported by whole-core data from the field area.

The Woodbine succession gradually thins from the axis of the East Texas Basin eastward to the Sabine Uplift. No more than the oldest 5 fourth-order Woodbine sequences (S1–S5) were ever deposited in the area of the Sabine Uplift, and only the oldest 3 fourth-order sequences (S1–S3) of the lower Woodbine Group are preserved below the base-of-Austin unconformity in the ETOF. Detailed correlation of sequence-stratigraphic surfaces, mapping of principal sandstone bodies, and description of whole cores allowed interpretation of depositional facies and key depositional surfaces and provided corroboration of our regional sequence-stratigraphic interpretation.

The field's reservoir zones comprise two systems tracts: (1) a conglomeratic lowstand fluvial incised-valley system in the north and west parts of the field, and (2) generally lenticular sandstones within the underlying highstand deltaic succession that occurs throughout the field.

North Pilot Area (NPA)

Throughout the NPA in northern Gregg County (fig. 7), the S3 lowstand incised-valley fill overlies the S1 highstand and transgressive (Maness Shale) systems tracts (fig. 8). The lowstand deposits consist of multiple successions of chert- and quartz-clast conglomerates and conglomeratic-to-coarse sandstones that grade upward into fine-to-coarse sandstone (Hentz and Bonnaffé, 2010). These successions, represented in cores from several wells in the NPA, are interpreted to represent multistoried fluvial-channel deposits within the incised-valley interval (Ambrose and others, 2009). This interval, the field's primary reservoir, is termed the "main sandstone" by operators. The base-of-Austin unconformity truncates the top of the S3 incised-

valley fill across the NPA. The S1 highstand facies, referred to as Woodbine “stringer sands” by operators, exhibit a suite of sedimentary features typical of fluvial-dominated deltaic systems. Sandstones are typically fine-to-very fine grained. Cored intervals recording prodelta, delta-front, delta-plain, and distributary-channel facies dominate (Ambrose and others, 2009). Throughout the field, the S1 highstand deltaic interval was divided into three zones by four chronostratigraphic horizons (flooding surfaces): FS1, 2, 3, and 4 (fig. 8). FS4 is cut out by the S3 lowstand incised-valley fill (main sand) throughout most of the field. FS1, 2, and 3 define the stratigraphic zones upon which the gross-sandstone maps presented later in the report are based.

The entire S2 succession has been removed by the valley incision in the NPA. Regional sequence correlations show that erosion of the S2 interval characterizes the entire west margin of the ETOF (fig. 8). We infer that the erosion provides a record of increased regional downcutting to adjust to a lower base level created by the initial relative rise of the Sabine Uplift during early Woodbine (S3) deposition.

Sequence boundaries are the most significant Woodbine surfaces that define sandstone units and reservoir-facies trends in the ETOF (Hentz and Bonnaffé, 2010). In the NPA, these boundaries include SB10 at the top of the Buda Limestone (mid-Cenomanian unconformity [Salvador, 1991]), SB30 (base of incised-valley fill), and the base-of-Austin unconformity. SB30 marks the boundary between the field’s primary reservoir, the S3 lowstand incised-valley fill (“main sandstone”), from the underlying upward-coarsening highstand deltaic “stringer” zone—the primary completion target today. The distinctly erosional surface occurs as fluvial chert-clast conglomerate or coarse granular sandstone overlying distal-delta mudstones and siltstones, recording a pronounced drop in relative sea level. SB10, at the top of shelf deposits composing the Buda Limestone throughout the field and basin, is also interpreted to be a transgressive surface of erosion, although log data record no pronounced unconformity at the contact with the overlying transgressive Maness Shale. The base-of-Austin unconformity in the pilot areas, an inferred mid-Turonian, third-order sequence boundary and transgressive surface of erosion (Ambrose and others, 2009), marks the base of the top seal in the field. Primarily chert and milky quartz clasts derived from incised-valley-fill conglomerates of the underlying Woodbine were incorporated in the basal part of the transgressive Austin Chalk. Well-developed paleosols in the lower Woodbine facies immediately below the Austin contact in the south part of the field and in cores outside the field record a period of long-term subaerial exposure associated with this unconformity.

South Pilot Area (SPA)

The Woodbine section of the SPA occurs just east of the erosional limit of the S3 incised-valley-fill system in west-central Rusk County, which most likely coincides with its approximate depositional limit. Unlike the section in the NPA, therefore, the Woodbine interval in the SPA comprises only the S1 highstand deltaic “stringer” succession (MFS10 to SB20) (fig. 8). The same succession in the NPA exists between MFS10 and the base of the lowstand valley fill (SB30), and its thickness in the north varies according to differences in depth of valley incision. Moreover, the S1 highstand interval in the SPA is more complete and, therefore, comprises significantly more of the sequence’s uppermost reservoir-quality (generally thickest, coarsest grained), deltaic topset sandstones than in the NPA. The entire S1 highstand interval, the SB20 surface, and part of the transgressive systems tract at the base of S2 are generally preserved only in the western (downdip) part of the southern part of the field immediately below the base-of-Austin unconformity (fig. 8).

DEPOSITIONAL SYSTEMS

The Woodbine Group in the ETOF contains a lower highstand sequence composed of narrow and lenticular sandstones in a fluvially dominated deltaic system. These deltaic deposits are eroded and overlain by an upper section of Woodbine fluvial deposits composed of conglomerates and coarse-grained sandstone beds of lowstand incised-valley fill origin (fig. 7) (Ambrose and others, 2009; Ambrose and Hentz, 2010).

Highstand Fluvial-Dominated Deltaic System

Extreme sandstone body heterogeneity in the lower Woodbine Group is controlled by the fluvial-dominated deltaic depositional architecture, with dip-elongate (i.e., north–south oriented) distributary-channel sandstones pinching out over short distances (typically <500 ft [<150 m]) into delta-plain and interdistributary-bay siltstones and mudstones (figs. 9 and 10). Well-developed, dip-elongate sandstone bodies in fluvial-dominated deltaic systems define narrow distributary channels that bifurcate seaward, terminating in lenticular channel-mouth bars (Fisk, 1961; Frazier, 1967; Brown and others, 1973; Galloway, 1975; Neill and Allison, 2005; Olariu and Bhattacharya, 2006). These distributaries are commonly flanked by lobate and thin crevasse splays formed by levee breaching and subsequent infilling of muddy interdistributary bay and lower-delta-plain facies (Coleman and Gagliano, 1964; Elliott, 1974; Coleman and Wright, 1975; Olariu and Bhattacharya, 2006; Olariu and others, 2010). Sandstone-body continuity and sweep efficiency in fluvial-dominated deltaic reservoirs is typically poor to moderate because narrow distributaries and lobate crevasse splays are areally segregated within muddy delta-plain deposits (Coleman and Wright, 1975; Tyler and others, 1984; Tyler and Finley, 1991). Heterogeneity in fluvial-dominated deltas is also increased by variable distributary-channel fill, abundant soft-sediment deformation related to variably compactible facies belts, dewatering of delta-plain sediments, and development of peat swamps and paleosols (Frazier, 1967; Styan and Bustin, 1983; Fielding, 1985; Bhattacharya and Walker, 1992; Ryer and Anderson, 2004).

The Shell No. 55 Watson core (fig. 11) illustrates a complete stratigraphic succession of highstand deltaic deposits from the top of the Buda Limestone at 3,728 ft to an inferred unconformity at the base of lowstand incised-valley fill deposits at approximately 3,625 ft (fig. 12). Prodelta deposits represent relatively deepest water conditions (several tens of feet to >100 ft [Allison and Neill, 2002; Trincardi and others, 2003]) in the deltaic system. They comprise calcareous mudstone beds from approximately 3,710 to 3,725 ft in the Shell No. 55 Watson

core. They grade upward into distal-delta-front deposits consisting of very fine-grained sandstone beds intercalated with silty mudstone beds from 3,680 to 3,710 ft (figs. 12b and 12c). Overlying proximal-delta-front and delta-plain deposits, extending from 3,640 to 3,677 ft (figs. 12d and 12e), are coarser grained than the underlying deposits and contain abundant ripple-laminated, fine-grained sandstone beds and carbonaceous, silty mudstone layers.

The section from 3,640 to 3,677 ft is composed of splay-platform deposits, illustrated at approximately 3,660 ft by a 6-inch zone of massively deformed and mottled organic-rich mudstone with abundant carbonaceous filaments. This section is capped by a massively oil-stained, 10- to 15-ft section from 3,625 to 3,640 ft of fine- to medium-grained sandstone representing distributary-channel deposits truncating older crevasse-splay and splay-channel deposits (fig. 12a).

The incompletely recovered, coarse-grained upper part of the Shell No. 55 Watson core above 3,625 ft consists of chert- and quartz-clast conglomerates and variably oil-stained, medium- and coarse-grained conglomeratic sandstone beds; thin mudstone zones; and very fine-grained sandstone beds (figs. 12a, 12f, 12g). This upper section represents nonmarine, bedload fluvial deposits containing numerous mudstone-draped, gravelly sandbar deposits.

A gross-sandstone thickness map of the oldest highstand depositional interval defined in this study (FS1 to FS2) (fig. 13) illustrates south- and southwest-trending, narrow (<1,500-ft [<450-m]) belts of >15 ft (>4.5 m) of gross sandstone that define depositional axes of a fluvial-dominated deltaic system. Gross-sandstone contours in the south part of the study area are dominated by southward-bifurcating patterns, recording small-scale distributaries with sandy lobate channel-mouth-bar deposits at the point of bifurcation. These channel-mouth-bar deposits are the sandiest part of the system and commonly contain >20 ft (>6 m) of gross sandstone. In contrast, sandstone body geometry in the FS1-to-FS2 interval in the northern part of the field contains anastomosing and tributary patterns, consistent with mud-rich fluvial systems in a lower-delta-plain setting (see the fluvial classification scheme of Galloway [1977] wherein mud-rich fluvial systems are commonly anastomosing). The channel-fill depositional framework in the northern part of the field is defined by narrow (commonly 1,000- to 1,500-ft [305- to 450-m]), moderately sinuous belts of >10 ft (>3 m) of gross sandstone.

The overlying FS2-to-FS3 interval displays gross-sandstone thickness patterns that are similar to those of the FS1-to-FS2 interval (fig. 14). Narrow (commonly <1,500-ft [<450-m]), moderately sinuous belts of >20 ft (>6 m) of gross sandstone in the northern part of the field

represent lower-delta-plain channel systems that grade downdip (south and southwestward) into southward-bifurcating belts of >20 ft (>6 m) of gross sandstone, recording fluvial-dominated distributaries that pinch out laterally into muddy interdistributary-bay deposits with <10 ft (<3 m) of gross sandstone.

Lowstand Incised-Valley System

The lower highstand section is truncated in the northern and western parts of the field by a thick (commonly 100- to 150-ft [30- to 45-m]) lowstand, valley-fill succession composed of bedload fluvial deposits of multistoried coarse-gravel and coarse-grained sandy beds. This valley-fill section in some areas of the ETOF directly overlies muddy, delta-front deposits, from which as much as 100 ft (30 m) of lowstand incision is inferred. This upper section, termed the "main sand" by field operators, accounts for most of the field's primary production. Early significant oil production from the main sand resulted in rapid upward migration of oil–water contacts. Strategies employed to maximize oil production and to limit upward migration of oil–water contacts include plugging lower, water-producing zones and recompleting zones of oil-saturated, coarse-grained sandstones bounded by thin (<5-ft [<1.5-m]) interchannel mudstones (Wang, 2010).

Channel-fill successions of modern bedload fluvial deposits are commonly composed of sandy or gravelly longitudinal and transverse bars that form by downstream migration in braided-river systems (fig. 7a). Most channel-fill deposits in these coarse-grained fluvial systems formed by channel-floor migration of coarse-grained sand and gravelly sand bars (Galloway, 1977; Allen, 1983; Lunt and others, 2004). Downstream accretionary bars are characteristic of braided streams and are typically ≤3 ft high, tens of feet wide, and hundreds to thousands of feet long (Miall, 1992). These coarse-grained bars are commonly draped by fine-grained material deposited during slack-water suspension sedimentation between periods of flashy sediment discharge (Rust, 1972; Miall, 1985). Lateral continuity in individual bedload-fluvial channel-fill sandstone beds is variable but can be great in large composite channel fills (Galloway, 1977; Schumm, 1981). Vertical continuity in these systems can also be great where successive channel fills are amalgamated into multistoried sandstone bodies.

A short 30-ft core from the ARCO No. B142 King well (fig. 11) includes parts of all three major stratigraphic intervals in the ETOF, from base to top: (1) lower Woodbine deltaic stringers, (2) the upper incised-valley-fill interval, and (3) the basal 3.5 ft of the Austin Chalk. A 10-ft section of the lower Woodbine stringer interval, composed of thin (<4-in) beds of very fine-

grained sandstone interbedded with burrowed mudstone, is truncated by a nonmarine, coarse-grained section of multistoried gravel-bar and sandy channel-fill deposits (figs. 15a–c). The upper incised-valley fill section consists of chert-clast conglomerate layers interbedded with planar-stratified and crossbedded medium–to–coarse-grained sandstone beds (fig. 15d). Multiple erosional surfaces in the section record successive cannibalization of channel-floor bars, resulting in a nonsystematic grain-size profile, although only 18 ft of the upper valley fill is preserved below the base-of-Austin-Chalk unconformity (fig. 15a). This unconformity, the main seal for hydrocarbons in the field, is directly overlain by a 1- to 2-ft zone of pebble and small-cobble rip-up clasts from the underlying Woodbine section. Abundant shell fragments are also present, recording marine transgression over an exposed Woodbine surface. The lower Austin Chalk section is well cemented with calcite and represents a permeability barrier at the top of the Woodbine stratigraphic section.

A gross-sandstone thickness map of the lowstand incised-valley section shows broad, sheetlike patterns and gradual, eastward thinning from >140 ft (>43 m) to <20 ft (<6 m) of gross sandstone (fig. 16). Gross-sandstone contours in this map are relatively nonsinuous and subparallel, although sinuous patterns occur in the northwest part of the map area, where most of the interval is preserved below the base-of-Austin-Chalk unconformity.

FIELD TESTS AND RESULTS

The field-demonstration tests started in August 2010. The scope of tests included workover, deepening/recompletion, and miniwaterflooding. Sixty wells in Danmark Energy LP and Linder Operating Co. leases around the Castleberry Survey were selected (fig. 17). Different from the main Woodbine sandstone, stringer sandstones are laterally discontinuous, lower-quality reservoirs with relatively low porosity, low permeability, and low resistivity. Some stringers with low resistivity looked wet but produced oil without water. Resistivities determined from logs of new deep Cotton Valley Sand gas wells in the area, showing the wet conditions of lower stringers, are the best indicators for locating deepening and recompletion targets. In areas without new deep wells, deepening targets were selected according to the depositional trends determined from logs in older wells.

Criteria used for ranking recompletion targets were (1) intervals with fair-to-good GR or SP responses and resistivity values greater than 2 ohm-m, (2) deepened-but-not-produced targets, (3) wells producing less than 3 bbl/d, (4) sufficient baffle between the upper S2 stringer sandstone and the overlying main Woodbine sandstone, and (5) thickness.

The S2 stringer in the northern area is deposited in a distributary channel of the deltaic succession. In some places, the distributary channels, difficult to differentiate from the main Woodbine fluvial channels, have been considered as part of the main-sand Woodbine by operators. The quality of S2 sandstone varies considerably in both vertical and lateral directions. Most of the high-quality S2 sandstones were already produced; in this study, we were targeting locally compartmentalized low-quality S2 sandstones. One of the challenges in producing S2 sandstones has been to differentiate the compartmentalized (prospective) S2 sandstones from the produced (wet) S2 sandstones. In addition, to successfully produce from S2 sandstone, the S2 sandstone needs to be separated from the main Woodbine geologically and mechanically. If the baffle between the upper S2 stringer sandstone and the overlying main Woodbine sandstone is not sufficient, it could be difficult to block water from the main Woodbine sandstone, which hampers oil production from the S2 stringer sandstone.

The lower S1 stringer sandstone is a distal deltaic system. It comprises highly compartmentalized, low-quality sandstone with low porosity and permeability. Vertically, it can be separated from the upper S2 stringer sandstone with a thick shale baffle. It is better-developed in Phase II and III areas than in the Phase I area. For instance, a thick, medium-quality S1 sandstone was developed in the updip South Kilgore Unit (SKU). Although the quality

of S1 stringer sandstone is generally poor, it has good potential to produce oil with zero-to-little water for several years. The criteria used in selecting targets in S1 stringer sandstone are to better identify quality sandstones and to identify those with >2 ohm-m resistivity values.

Fifteen targets were selected and ranked (table 4 and open asterisks in fig. 17). Ten of these targets (solid asterisks in fig. 17) were tested between July 2010 and July 2011, and five were tested in 2012. The cost of each test ranged from $8,500 to $135,000 (table 4), with a total close to $1 million, which was $300,000 more than the $700,000 of cost share required by RPSEA. Results of these tests are summarized in table 4 and fig. 18.

Boston Moore "A" Lease

The Boston Moore "A" Lease is a small lease adjacent to the Dolly Bell Key Lease, which was selected for a miniwaterflooding test and would be one of the producers for the miniwaterflooding pilot. Wireline logs show a 15-ft S1 stringer sandstone and a 10-ft S2 stringer sandstone with high resistivity values. The S2 sandstone was tested with 122 bbl/d in 2003; by August 2010, the well produced 1.1 bbl/d with 263 bwpd. Danmark cleaned the well and reperforated the S2 sandstone at a cost of $24,000. Production increased to 10 bbl/d with a high watercut and declined slightly to 7.2 bbl/d with 94 bbl of water in August 2012. The workover was paid out in a month and produced ~5,000 STB as of August 2012.

Boston Moore "B" Lease

The Boston Moore "B" Lease is one of the leases with a good production rate in 2010. It was selected because it has not only good potential in stringer sandstones but also an unusual production history. The S2 stringer sandstone is well developed, with a thickness ranging from 5 to 15 ft (fig. 19). Many wells in the lease were produced from lower stringers since the 2000's. Two adjacent wells, Boston Moore "B" #s 9 and 10, were deepened in 1995. Wireline log data showed that the entire main Woodbine in #10 was completely wet but that the lower part of main Woodbine in #9 was only partially wet. The S2 stringers are 10 ft thick in #9 and 15 ft thick in #10, with >2 ohm-m in resistivity values, which suggests a high likelihood that they were not flooded. Although S2 in well #10 is thinner than in #9, the GR log suggests that the quality of S2 sandstone in well #10 is better than that of #9. With a production rate of 36 bbl/d in November 2010, well #10 is the best producer in the lease.

The S2 stringer in #9 was perforated in 2005 and produced at an initial rate of 36 bbl/d with 62 bbl of water. By April 2010, the production declined to 13 bbl/d, and in August 2010,

Danmark repaired the pump at a cost of $8,500. The production increased from 13 to 24 bbl/d and peaked at 50 bbl/d in December 2010. The well was tested at 24.4 bbl/d in February 2012 and at 17 bbl/d in October 2012. The incremental production and revenue have been approximately 16,000 STB and $1.5 million—a 180x multiplier on the cost to repair the pump.

Boston Moore “B” #2 is a very interesting well. It produced at an average rate of 5 bbl/d from 2000 to 2007 before dropping to 1.4 bbl/d in August 2007. Then, production increased gradually and peaked at 31 bbl/d in August 2010. It was tested at 10 bbl/d with 71 bbl of water on March 6, 2012. The reason for the production increase from 2007 to 2010 is not clearly known. The improvement might have been caused by an increase in reservoir pressure from increased water injection, or perhaps there was an increase in permeability around the well.

A similar production increase was also noted in Boston Moore “B” #s 10 and 14. Production from #14 was increased from 8.4 to 17.5 bbl/d in August 2010, peaked at 30.1 bbl/d in January 2012, and decreased to 15.8 bbl/d in June 2012, with a fairly constant water cut of 84%. The well was reperforated in late June 2012, and production increased from 15 to 29.5 bbl/d with a water cut of 79%.

The Boston Moore “B” #17 was one of the shallow wells completed only to the main Woodbine and had been shut in since 2001. Fig. 19 indicates that the S2 stringer in the area could be ~10 ft thick, and the well was deepened and recompleted in the upper S2 stringer. It was tested at 13 bbl/d with 1.5 bbl of water on September 23, 2012.

Matt Moncrief Lease

With a cumulative production of over 15 MMSTB as of January 2014, the Matt Moncrief Lease is one of the best-produced leases in the Castleberry Survey (fig. 20). Of 72 wells, 41 are still active. The S2 stringer sandstone is present, with an average thickness of >10 ft (fig. 21) in part of the lease. However, reservoir quality of S2 sandstone changes quickly in both lateral and vertical directions (fig. 21). Most higher-quality S2 sandstones have been produced and the locally compartmentalized, medium–to–low-quality S2 sandstones are targets for deepening and recompletion.

Deepening and recompletion have increased the lease production since 2004. In 2003, TXOK drilled a deep gas well (Moncrief #3) between Moncrief #s 47 and 55. Resistivity values of >2 ohm-m suggest that the 20-ft thick S2 distributary channel was possibly not produced (fig. 21). In 2004, Moncrief #47 was recompleted and encountered an 18-ft S2 stringer. It was tested

with an initial rate of 69 bbl/d without water, and production declined gradually to 7.3 bbl/d with only 39 bbl of water in April 2012. As of June 2014, this recompletion has produced approximately 80,000 STB of oil. In October 2007, Moncrief #s 12 and 43 were recompleted in the S2 stringer. Moncrief #12 encountered a low-quality S2 stringer with only 3 ft of sand at the top and over 2 ohm-m in resistivity. Although it was tested with an initial rate of 43 bbl/d (Nault, oral commun., 2008), the production declined quickly and only lasted for several months. On the other hand, Moncrief #43 encountered a 14-ft good-quality S2 stringer. It was tested with an initial rate of 58 bbl/d, and production declined to 13.5 bbl/d with 201 bbl of water in March 2012.

Figure 21 shows a 14-ft-thick (3618 to 3632 ft) distributary channel (S2) with good resistivity in the Moncrief #38 well. This S2 sandstone is separated from the main Woodbine channel by a 3-ft-thick shale baffle. This well was deepened in 1982, and the good production from the main Woodbine had excluded it from recompletion for 28 years. In August 2010, the production of 5 bbl/d from the main Woodbine made it a low-priority well for recompletion. With the first three unsuccessful recompletions in 2010, Danmark recompleted the well in the lower S1 stringer sand in February 2011 at a cost of $35,000, with an initial production of 79 bbl/d without water. As of June 2012, this recompletion produced >22,000 STB and >$2.0 million in revenue. With a EUR of 27,000 STB, estimated revenue will be $2.5 million, which will result in a 70-fold profit—the best recompletion in this study. The good GR and resistivity in the lower S1 sandstone (20-ft thick) is a candidate for future recompletion.

Because there was no earlier deepening in the vicinity of Moncrief #28 (fig. 21) and it had the potential to open up additional opportunities in the northern area, #28 became one of the high-priority locations in the Moncrief lease for the S2 recompletion. It was deepened in March 2011 at a cost of $75,000. Although #28 encountered a 20-ft high-quality watered-out distributary channel, it nevertheless provided valuable information on the S2 stringer and supports our theory that most high-quality S2 distributary channels are fully or partially connected to the main Woodbine and have been flooded (wet).

Moncrief #22, located in the western part of the Moncrief Lease (fig. 20), had been recommended for deepening and recompletion for the upper S2 stringer since 2007 in our earlier study (Wang and others, 2008). However, the >3 bbl/d from the main Woodbine had excluded it from recompletion for many years. In July 2011, production fell to 2.5 bbl/d, and the #22 was deepened and recompleted in the S2 sand with an initial production of 40 bbl/d without water at a cost of $135,000. The cost of this recompletion was paid out in 40 days, and as of

June 2012 has produced >11,000 STB and >$1 million in revenue. With an EUR of 17,000 STB, estimated revenue will be $1.5 million.

To explore the potential of the S2 stringer near the Moncrief #38, Moncrief #s 13 and 53 were deepened in October 2012, albeit unsuccessfully because of mechanical problems.

J. W. Akin Lease

The J. W. Akin Lease is located south of the southeast part of the Matt Moncrief Lease. A deep gas well, Shell J. W. Akin #24, completed in 1994, showed a 15-ft S2 stringer sandstone (fig. 21) with good resistivity, which suggested that the S2 sandstone in this area was good for recompletion. The Akin #1 well was deepened and recompleted in August 2010 at a cost of $95,000. Because of the problem of separating from the main Woodbine reservoir, Akin #1 was tested with 100% water; Danmark then decided to recomplete the nearby Akin #10 well. Akin #10 was deepened and recompleted in the 18-ft-thick S2 stringer (fig. 21) in March 2011 at a cost of $92,000. It was tested with 39 bbl/d and declined to 26 bbl/d in March 2012. The cost of this recompletion was paid out in 30 days; as of March 2012, the recompletion produced approximately 12,000 STB and >$1 million in revenue. With a EUR of 25,000 STB, estimated revenue will be $2.2 million.

Akin “B” Lease

Similarly, a deep gas well completed in 2003 showed a 20-ft S2 stringer sandstone with good resistivity, suggesting that the S2 sandstone in this area was good for recompletion. The Akin “B” #15 well was deepened and recompleted in August 2010 at a cost of $101,000 and tested 100% water.

Bumpas-Bassham Area

Bumpas and Bassham leases have been selected because Bumpas “C” #12 was deepened in 2007 and encountered a 22-ft S2 stringer. It was recompleted with an initial rate of 125 bbl/d without water in 2007 (Nault, oral commun., 2008); by March 2013, it still produced at 17 bbl/d with 124 bbl of water. A deep Cotton Valley Sand gas well, Kutch GU #3, was completed in 2005 and showed a 15-ft S2 stringer sandstone (fig. 22). The >2 ohm-m resistivity suggested the S2 stringer in this area was good for recompletion. Bassham #s 4, 8, and 9 produced less than 0.3 bbl/d with >300 bbl of water from the main Woodbine. Bassham #8 was

deepened and recompleted in the S2 stringer in October 2012 and tested with an initial rate of 54 bbl/d. By June 2014, we estimate that it had produced over 15,000 STB of oil.

Spurrier-Turner Area

The Turner Lease was selected because Spurrier wells #3 and #6 (fig. 23a) were recompleted in the S2 stringer in 1996 and 1997. Production increased from 500 to 1600 barrels of oil per month (fig. 23b). The S2 stringer was expected to be present in the Turner Lease (fig. 23c). Turner #16 was recompleted in September 2010; it tested with 100% water because the recompletion was actually in the main Woodbine instead of in the stringer sands. Turner #15 was deepened and recompleted in the 30-ft-thick S1 and S2 stringers (fig. 23c) in May 2011 at a cost of $105,000. It was tested at 13 bbl/d and 148 bwpd; production declined to 3.5 bbl/d with 370 bbl of water in April 2012. Despite the low oil rate and high watercut, the recompletion was paid out in 4 months. The low oil rate and high watercut suggest the stringers in this area are connected to the downdip aquifer and have been affected by the S2 stringer production on the Spurrier Lease.

LABORATORY TESTS ON SURFACTANT/POLYMER AND CO_2 FLOODINGS

Both surfactant/polymer and carbon dioxide (CO_2) floodings were tested in the laboratory using the ETOF and Berea sandstone cores to determine the feasibility of these processes for recovering a portion of the 1.1 billion STB of residual oil in the ETOF. The laboratory tests, using crude oil from the ETOF, were carried out by the Tertiary Oil Recovery Program at the University of Kansas.

The CO_2 displacement study consisted of measurements of fluid properties, phase behavior observations, core sample characterization, and core flow tests to estimate recovery efficiency with CO_2 injection. The miscible mechanisms of CO_2 flooding (fig. 24) include CO_2 condensation and oil vaporization. After CO_2 is dissolved into oil, oil components are vaporized into CO_2 and a pure CO_2 zone.

A 38-ft-long slim tube was used for the CO_2 displacement test. Five tests were conducted at a reservoir temperature of 146°F, with pressures varying from 1568 to 2057 psi (fig. 25). The MMP was determined as the pressure at which the recovery reaches 90% when 1.2 hydrocarbon pore volume (HCPV) of CO_2 is injected. Figure 26b shows the oil recovery results.\. At 1.2 HCPV of CO_2 injection the MMP (the pressure at 90% of oil recovery) is estimated as 1776 psi, which is slightly lower than the 1850 psi estimated by Wang (2008).

Core flow tests were conducted using Berea sandstone and ETOF reservoir core plugs. Core plugs from the Woodbine reservoir were taken from the Key Lawson #1 well in the adjacent aquifer in Upshur County, Texas. All the core plugs were 1 inch in diameter and 3–4 inches in length. The core properties are listed in tables 5 and 6. Note that porosity and permeability values of cores from this dry well are significantly lower than those in the ETOF.

Figure 26a shows the swelling/extraction curve for the oil/CO_2 system at 146ºF with 3 cc of sample (12% volume of cell volume). CO_2 solubility is also plotted in the same figure as a function of pressure. The swelling factor of oil is the ratio of volume at reservoir conditions to volume at stock-tank conditions. This swelling factor was determined by measuring the change of interface level as a result of CO_2 dissolution in the oil. CO_2 solubility was calculated based on the assumption of a negligible hydrocarbon component in the vapor phase. Maximum swelling occurred at 1464 psi, when oil volume was 1.22 of its original volume, with 0.67 mole fraction of CO_2 dissolving in the liquid phase. Extraction appears to have started at approximately the same pressure. As pressure increased, oil volume continued to shrink and CO_2 extracted more hydrocarbon components from the liquid phase. The rate of oil volume shrinking by extraction

was faster than the rate of swelling by continued dissolution of CO_2. At 2615 psi, the oil volume shrank by as much as 33% of its original volume.

Each core was waterflooded to residual fluid saturation, and carbon dioxide was injected at 0.1 cc/min to recover the residual oil in the core. The results of tertiary CO_2 flooding in different cores are summarized in tables 7 and 8.

The recovery efficiency of remaining oil in place (ROIP) increases from 52% to 90% on Berea sandstone core and from 24% to 70% on ETOF core when pressure increases from 1100 to 2000 psi (fig. 27). Significantly lower recovery efficiencies in the ETOF core than in the Berea core, although not clearly understood, might have stemmed from differences in clay type and content in these cores.

At current pressure of 1,000 psi in the ETOF, the recovery efficiency of CO_2 injection will be about 20%. Increasing recovery efficiency to 70% requires increasing the reservoir pressure to 1,780 psi, and casing leaks will be a major consideration. In a 1972 study, one quarter of wells in the ETOF had casing leaks (fig. 28). With most wells over 80 years old, leaking of CO_2 will be an environmental and economic issue that is difficult to overcome. In addition, the issue of CO_2 containment and the low residual oil saturation (table 2) of 14% in the main Woodbine reservoir lower the efficiency of CO_2 utility and can make the CO_2 flooding economically unfavorable.

Summary of Laboratory-Based CO_2-EOR Testing

1. From the slim-tube experiments, MMP was estimated to be 1776 psi at a reservoir temperature of 146°F. At current reservoir pressure, 1100 psi, any carbon-dioxide injection process would result in an immiscible displacement.
2. The maximum swelling factor of ETOF crude oil with CO_2 is 1.22 at 1464 psi and 146°F. At current reservoir pressure, the swelling factor is 1.16.
3. Dissolution of CO_2 into crude oil reduces the viscosity of the oil as much as a factor of 5 when the pressure is above 1500 psi. At current reservoir pressure, the viscosity-reduction factor is 3.
4. When CO_2 was injected at pressure above the MM, more than 60% of the waterflood residual oil from reservoir core and Berea sandstone was recovered. At the current

reservoir pressure in the ETOF, the displacement process is immiscible and the recovery from the remaining oil in place would only be in the range of 24%.

Alkaline-Surfactant-Polymer (ASP) Flooding

A feasibility study was conducted on the application of chemical (alkaline-surfactant-polymer) flooding to the ETOF. The principal objectives were to identify efficient alkaline-surfactant-polymer formulations for the ETOF crude oil from phase behavior studies and to examine, via flow tests through ETOF cores, the performance of the chemical formulations when recovering residual oil. Five chemical formulations were tested by phase behavior studies; different formulations were mixed with crude oil and then allowed to equilibrate at the reservoir temperature. Each chemical formulation with ETOF crude oil achieved optimal salinity.

Phase Behavior Studies

Phase behavior studies were conducted to identify chemical formulations that are capable of producing oil from waterflooded reservoirs. Selected chemical systems containing surfactants, cosolvents, polymers, and so on were prepared in a salinity scan, a series of solutions where only the salinity is varied. Optimum salinity exists when equal amounts of water and oil are solubilized and the interfacial tensions (IFT) between the middle-phase microemulsion with both the water and oil phases are the lowest (fig. 29). Chemical floods are usually designed with the chemical formulation injected at optimum salinity in order to have the highest oil-recovery performance.

Surfactants used and reported here were Petrostep S-13D [alcohol propoxy sulfate; Stepan Company], Petrostep S2 [internal olefin sulfonate, Stepan Company], Cedepal FA-406 [ammonium alkyl ether sulfate, Stepan Company], Neodol 25-12 [alcohol ethoxylate, Shell Chemical Company], and Novel TDA-12 Ethoxylate [ethoxylated alcohol, Sasol North America, Inc.]. The cosolvent, or alcohol, used was sec-butanol. The polymers used were Flopaam 3330s [polyacrylamide; 25% hydrolysis; 8 million Dalton; SNF, Inc.] and Flopaam 3530s [polyacrylamide; 25% hydrolysis; 16 million Dalton; SNF, Inc.].

Four ASP systems were formulated with different surfactant, cosurfactant, and sodium bicarbonate content (fig. 30). The effect of alkaline-sodium bicarbonate is to reduce adsorption of surfactants at reservoir rock surfaces. Decreasing the ratio between Petrostep S-13D and Petrostep S2 leads to a higher optimum salinity. Using less alcohol usually produces a higher optimum salinity.

Corefloods

Two types of chemical systems were selected for core tests. System 1 contained an alcohol propoxy sulfate and an internal olefin sulfonate, with sec-butyl alcohol as a cosolvent. An alcohol ethoxylate and an ammonium alkyl ether sulfate were used as additives to this system to increase the optimal salinity of formulations. System 2 contained an alcohol propoxy sulfate and an ethoxylated alcohol and ammonium alkyl ether sulfate, and was prepared in synthetic field brine without alcohol. The selected systems did not contain alkali since the total acid number of the ETOF crude was low.

Three out of nine core plugs from the ETOF with higher permeabilities—#s 6, 8, and 9—were used in corefloods (fig. 31). Seven corefloods were tested: four on Berea cores and three on ETOF cores (table 9).

Performance of System 1 was initially tested in Berea sandstone cores; only three ETOF core plugs had sufficient permeability for core testing. Tracer tests showed much larger mixing zones in the ETOF core plugs as compared to the Berea sandstone. Tertiary oil recoveries in Berea sandstone were about 90%, indicating the efficiency of the selected formulations, while oil recoveries of about 28% were measured in ETOF core plugs (fig. 32). The impact of the mixing and/or retention of chemicals in the ETOF core plugs is thought to be the cause of the lower recoveries in the ETOF rock. The degree of retention of surfactants varies with the type and content of clay minerals in the rocks. The types of clay minerals in the ETOF are different from those in Berea cores, and the content of clay in ETOF cores can be significantly higher.

Summary of Laboratory-Based Alkaline-Surfactant Testing

- Five alkaline-surfactant-polymer (ASP) systems were formulated using ETOF crude oil; low interfacial tension in three phases was achieved in all five systems. The optimal salinity increased with the addition of nonionic surfactant Neodol 25-12 from Shell Oil Co. but decreased with the addition of the cosurfactant, sec-butanol alcohol.
- The effect of alkaline-sodium bicarbonate is to reduce adsorption of surfactants at reservoir rock surfaces.
- Oil recovery by ASP flooding in Berea and ETOF cores is 90% and 28%, respectively. Significantly lower oil recovery from ETOF cores than from Berea cores might have stemmed from the high adsorption of surfactants by clay minerals and the fact that optimal three-phase conditions were not achieved in the core flooding.

- More lab tests will be needed to find the optimal compositions for the ETOF.

Impact on Small Producers

Eight out of fifteen workover/deepening/recompletion tests were successful, and as of June 2014, more than 140,000 STB had been produced from these tests, with an EUR of ~210,000 STB. These workover/recompletions have generated more than $13 million in additional revenue. Pump repair, cleaning, and reperforation, all significantly improving well productivity, are the most routine and economical workovers for enhancing production of mature fields. Deepening and recompletion guided by depositional trends—low cost, low risk, and highly profitable—are also economically viable techniques for maximizing recovery from mature fields. In addition to Danmark, other operators such as BASA have also deepened many wells in the last several years. Collectively, these efforts have halted field decline and sustained production at ~11,000 bbl/d since 2010, while the number of producing wells has declined from 3,895 to 3,886.

TECHNOLOGY TRANSFER EFFORTS

The technology transfer of our findings, focused on the small operators in the ETOF, has been achieved through multiple efforts. Meetings with Danmark and Linder have been a key for the success of field tests; in turn, our efforts helped these companies identify correct stringer locations and prevented them from recompleting less prospective intervals or locations. Technology transfer was also carried out through publications, conferences, and workshops.

Articles and Reports

1. Hentz, T., Bonnaffé, F., Ambrose, W., Loucks, R., and Wang, F., 2010, Sequence stratigraphy, depositional facies, and reservoir attributes of the Upper Cretaceous Woodbine Group, East Texas Field, Texas: The University of Texas at Austin, Bureau of Economic Geology Report of Investigations No. 270, 124 p.
2. Dokur, M., 2012, Reservoir characterization of the Upper Cretaceous Woodbine Group in northeast East Texas Field, Texas, The University of Texas at Austin, Master's thesis, 98 p.

Conference and Workshop Presentations

Wang, F., Development strategies for maximizing East Texas oil-field production, presented at:

RPSEA Onshore Production Conference, Midland, Texas, April 10, 2012.
TIPRO, Kilgore, Texas, May 9, 2012.
ETEA Annual Meeting, Kilgore, Texas, Oct. 24, 2012.
RPSEA Onshore Production Conference, Houston, Texas, Nov. 29, 2012.
RPSEA Onshore Production Conference, Houston, Texas, Sept. 25, 2013.

Wang, F., Comparison between East Texas Oil Field and Daqing Oil Field, Workshop for Research Institute of Petroleum Exploration and Development, PetroChina, Oct. 18, 2010, Austin, Texas.

CONCLUSIONS

With current and ultimate recovery efficiencies of 78% and 80%, the East Texas Oil Field is one of the best giant oil fields. Production has been predominantly from the upper main Woodbine fluvial channel sandstone and, to a lesser degree, from the highly compartmentalized lower stringer sandstones, which have been difficult to locate. Depositional trends and reservoir architectures of lower S1 and S2 sandstones were mapped to help operators better locate their deepening/recompletion targets and design waterfloods.

Guided by these depositional-trend maps, Danmark conducted 15 workover/deepening/recompletion tests from 2010 to 2012; 8 of these were successful. As of June 2014, more than 140,000 STB had been produced from these tests, with an EUR of ~210,000 STB. These workover/recompletions have generated more than $13 million in additional revenue. Deepening and recompletion guided by depositional trends—low cost, low risk, and highly profitable—is an economically viable technique for maximizing recovery from mature fields. In addition to the success of Danmark, other operators such as BASA have also deepened many wells in the last several years. Collectively, these efforts have halted the field decline and sustained the production at ~11,000 bbl/d since 2010, while the number of producing wells has declined from 3,895 to 3,886.

Laboratory Tests showed that recovery efficiencies from CO_2 and ASP floodings were lower in ETOF cores than in Berea cores. Although 70% of the remaining oil can be recovered by a miscible CO_2 injection, low residual oil saturation and casing leaks are major factors affecting the feasibility of CO_2 injection in the ETOF. The unexpected low recovery efficiency of 30% made the ASP flooding highly unfavorable for the ETOF.

RECOMMENDATIONS

This study covered two-thirds of the ETOF. It would benefit the operators a great deal if the entire field could be studied and mapped. Different compositions of surfactant/polymer systems should be tested and cores analyzed for clay content to determine the reasons for the low recovery efficiency from alkaline/surfactant/polymer compositions used in this study.

REFERENCES

Allen, J. R. L., 1983, Studies in fluviatile sedimentation: bars, bar complexes and sandstone sheets (low-sinuosity braided streams) in the Brownstones (L. Devonian), Welsh Borders: Sedimentary Geology, v. 33, p. 237–293.

Allison, M. A., and Neill, C. F., 2002, Accumulation rates and stratigraphic character of the modern Atchafalaya River prodelta, Louisiana: Gulf Coast Association of Geological Societies Transactions, v. 52, p. 1031–1040.

Ambrose, W. A., and Hentz, T. F., 2010, Depositional systems and facies variability in highstand fluvial-dominated deltaic and lowstand valley-fill systems in the Lower Cretaceous (Cenomanian) Woodbine Group, East Texas field: The University of Texas at Austin, Bureau of Economic Geology Report of Investigations No. 274, p. 17–81.

Ambrose, W. A., Hentz, T. F., Bonnaffé, F., Loucks, R. G., Brown, L. F., Jr., and Wang, F. P., 2009, Sequence stratigraphic controls on complex reservoir architecture of highstand fluvial-dominated deltaic and lowstand valley-fill deposits in the Woodbine Group, East Texas field: regional and local perspectives: American Association of Petroleum Geologists Bulletin, v. 93, no. 2, p. 231–269.

Ambrose, W. A., Hentz, T. F., Loucks, R. G., Frébourg, G., and Potter, E. C., 2014, Core workshop, Upper Cretaceous (Cenomanian) Woodbine Group, East Texas field, *in* Ambrose, W. A., Hentz, T. F., Loucks, R. G., Frébourg, G., and Potter, E. C.: Core workshop: sequence stratigraphy, depositional systems, and facies complexity in the Woodbine Group in East Texas field: The University of Texas at Austin, Bureau of Economic Geology, Workshop No. SW0020, 26 p.

Anonymous, 2003, Thomas D. Barrow—a legend in wildcatting: The Leading Edge**,** v. 22, no. 12, p. 1218–1222.

Bhattacharya, J. P., and Walker, R. G., 1992, Deltas, *in* Walker, R. G., and James, N., eds., Facies models: response to sea level change, Geological Association of Canada, p. 157–177.

Brown, L. F., Jr., Cleaves A. W., II, and Erxleben, A. W., 1973, Pennsylvanian depositional systems in north-central Texas: The University of Texas at Austin, Bureau of Economic Geology Guidebook No. 14, 122 p.

Casey Engineering Inc., 1994, Woodbine Sand, East Texas Field: Reservoir Engineering Report, Houston, Texas.

Coleman, J. M., and Gagliano, S. M., 1964, Cyclic sedimentation in the Mississippi River delta plain: Gulf Coast Association of Geological Societies Transactions, v. 14, p. 67–80.

Coleman, J. M., and Wright, L. D., 1975, Modern river deltas: variability of processes and sand bodies, *in* Broussard, M. L., ed., Deltas: models for exploration: Houston Geological Society, p. 99–149.

East Texas Engineering Association, 1953, The East Texas Field, 1930–1950: Internal Report, Kilgore, Texas, 621 p.

East Texas Engineering Association, 1972, Casing Corrosion Report: Internal Report, Kilgore, Texas.

Elliott, T., 1974, Interdistributary bay sequences and their genesis: Sedimentology, v. 21, p. 611–622.

Fielding, C. R., 1985, Coal depositional models and the distinction between alluvial and delta plain environments: Sedimentary Geology, v. 42, p. 41–48.

Fisk, H. N., 1961, Bar finger sands of the Mississippi Delta, *in* Peterson, J. A., and Osmond, J. C., eds., Geometry of sandstone bodies—a symposium, 45th Annual Meeting, Atlantic City, NJ: American Association of Petroleum Geologists Special Publication, p. 29–52.

Frazier, D. E., 1967, Recent deltaic deposits of the Mississippi River: their development and chronology: Gulf Coast Association of Geological Societies Transactions, v. 17, p. 287–315.

Galloway, W. E., 1975, Process framework for describing the morphological and stratigraphic evolution of deltaic depositional systems, *in* Broussard, M. L., ed., Deltas: models for exploration: Houston Geological Society, p. 87–98.

Galloway, W. E., 1977, Catahoula Formation of the Texas Coastal Plain—depositional systems, composition, structural development, ground-water flow history, and uranium distribution: The University of Texas at Austin, Bureau of Economic Geology Report of Investigations No. 87, 59 p.

Galloway, W. E., Ewing, T. E. Garrett, C. M., Jr., Tyler, Noel and Bebout, D. G., 1983, Atlas of major Texas oil reservoirs: The University of Texas at Austin, Bureau of Economic Geology, 139 p.

Gussow, W. C., 1973, East Texas field, the classic trap, has a new interpretation: Oil and Gas Journal, v. 71, no. 7, p. 134–136.

Hentz, T. F., and Bonaffe, F., 2010, Sequence stratigraphy of the Upper Cretaceous (Cenomanian) Woodbine Group: chronostratigraphic integration of the East Texas Basin and East Texas field, *in* Hentz, T. F., ed., Sequence stratigraphy, depositional facies, and reservoir attributes of the Upper Cretaceous Woodbine Group, East Texas field: Bureau of Economic Geology Report of Investigations No. 274, 114 p.

Levorsen, A. I., 1934, Relation of oil and gas pools to unconformities in the Mid-Continent Region: AAPG Bulletin, v. 18, p. 761–784.

Lunt, I. A., Bridge, J. S., and Tye, R. S, 2004, A quantitative, three-dimensional depositional model of gravelly braided rivers: Sedimentology, v. 51, p. 377–414.

Mancini, E. A., and Puckett, T. M., 2005, Jurassic and Cretaceous transgressive-regressive (T-R) cycles, northern Gulf of Mexico, USA: Stratigraphy, v. 2, no. 1, p. 31–48.

Miall, A. D., 1985, Architectural-element analysis: a new method of facies analysis applied to fluvial deposits: Earth Science Reviews, v. 22, p. 261–308

Miall, A. D., 1992, Alluvial models, *in* Walker, R. G., and N. James, N., eds., Facies models: response to sea level change: Geological Association of Canada, p. 119–142.

Minor, H. E., and Hanna, M. A., 1933, East Texas oil field: AAPG Bulletin, v. 17, no. 7, p. 757–792.

Minor, H. E., and Hanna, M. A., 1941, East Texas oil field: Rusk, Cherokee, Smith, Gregg and Upshur Counties, Texas, *in* Levorsen, A. I., ed., Stratigraphic Type Oil Fields, AAPG Special Publication 11, p. 600–640.

Neill, C. A., and Allison, M. A., 2005, Subaqueous deltaic formation on the Atchafalaya Shelf, Louisiana: Marine Geology, v. 214, p. 411–430.

Olariu, C., and Bhattacharya, J. P., 2006, Terminal distributary channels and delta front architecture of river-dominated delta systems: Journal of Sedimentary Research, v. 76, p. 212–233.

Olariu, C., Steel, R. J., and Petter, A. L., 2010, Delta-front hyperpycnal bed geometry and implications for reservoir modeling: Cretaceous Panther Tongue delta, Book Cliffs, Utah: American Association of Petroleum Geologists Bulletin, v. 94, p. 819–845.

Rust, B. R., 1972, Structure and process in a braided river: Sedimentology, v. 18, p. 221–245.

Ryer, T. A., and Anderson, P. B., 2004, Facies of the Ferron Sandstone, east-central Utah, *in* Chidsey, T. C., Jr., Adams, R. D., and Morris, T. H., eds., Regional to wellbore analogs for fluvial-deltaic reservoir modeling: The Ferron Sandstone of Utah: American Association of Petroleum Geologists Studies in Geology No. 50, p. 59–78.

Salvador, A., 1991, Origin and development of the Gulf of Mexico basin, *in* Salvador, A., ed., The Gulf of Mexico basin: Geological Society of America, Decade of North American Geology, v. J, p. 389–444.

Schumm, S. A., 1981, Evolution and response of the fluvial system, sedimentological implications, *in* Ethridge, F. G., and Flores, R. M., eds., Recent and ancient non-marine depositional environments: models for exploration: Society of Economic Paleontologists and Mineralogists (SEPM) Special Publication No. 31, p. 19–29.

Styan, W. B., and Bustin, R. M., 1983, Sedimentology of Fraser River delta peat deposits: a modern analogue for some deltaic coals: International Journal of Coal Geology, v. 3, p. 101–143.

Trincardi, F., Cattaneo, A., and Correggiari, A., 2003, Mediterranean prodelta systems: Oceanography, v. 17, no. 4, p. 34–45.

Tyler, N., and Finley, R. J., 1991, Architectural controls on the recovery of hydrocarbons from sandstone reservoirs, *in* Miall, A. D., and Tyler, N., eds., The three-dimensional facies architecture of terrigenous clastic sediments and its implications for hydrocarbon discovery and recovery: Society of Economic Paleontologists and Mineralogists (SEPM) Concepts in Sedimentology, v. 3, p. 1–5.

Tyler, N., Galloway, W. E., Garrett, C. M., Jr., and Ewing, T. E., 1984, Oil accumulation, production characteristics, and targets for additional recovery in major oil reservoirs of

Texas: The University of Texas at Austin, Bureau of Economic Geology Geologic Circular No. 84–2, 31 p.

Wang, F. P., Ambrose, W. A., Hentz, T. F., Bonnaffé, F., and Loucks, R. G., 2008, Engineering and geological characterization of giant East Texas oil field: north and south pilot studies: Society of Petroleum Engineers Paper No. 115683-PP, 15 p.

Wang, F. P., 2010, Engineering characterization of East Texas oil field: north and south pilot studies, *in* Hentz, T. F., ed., Sequence stratigraphy, depositional facies, and reservoir attributes of the Upper Cretaceous Woodbine Group, East Texas field: The University of Texas at Austin, Bureau of Economic Geology Report of Investigations No. 274, p. 95–114.

LIST OF TABLES AND FIGURES

Tables

Figures

sand") truncating lower section of deltaic deposits. Modified from Ambrose and others (2009) and Ambrose and Hentz (2010).

Figure 8. (a) Representative structural-dip cross section of the North Pilot Area (NPA), showing inferred fourth-order sequence stratigraphic surfaces and systems tracts. The datum is the base-of-Austin unconformity. No horizontal scale. (b) Representative structural-dip cross section of the South Pilot Area (SPA), showing inferred fourth-order sequence-stratigraphic surfaces and systems tracts. The datum is the base-of-Austin unconformity. No horizontal scale. GR = gamma ray; SP = spontaneous potential; Res = resistivity; SB = sequence boundary.

Figure 9. West–east structural cross section in the Kinney Lease in the SPA, showing location of producing and water-injection wells and complex deltaic facies architecture in the lower Woodbine (LWB) 30–40 interval (FS3 to FS4, this study) in the highstand deltaic succession. GR = gamma ray; Res = resistivity. Line of section is shown in figure 10a. Location of SPA shown in figure 11. From Ambrose and others (2009).

Figure 10. Sandstone thickness maps of two highstand deltaic stringer sandstone depositional units in the SPA in the southern part of the ETOF. (a) Net sandstone in the LWB 30–40 unit (FS3 to FS4, this study). (b) Net sandstone in the LWB 20–30 unit (FS2 to FS3, this study). LWB 20–30 and LWB 30–40 nomenclature is defined in Ambrose and others, 2009). (c) Monthly oil production in stock tank barrels (STB) from the Mason Lease from 1993 to 2007. Increased oil production in the Mason Lease (southwest corner of maps) in 1997 resulted from water injection into transmissive, southwest-trending distributary-channel sandstones in the LWB 30–40 unit. West–east structural cross section in the Kinney Lease is shown in figure 9. Location of SPA is shown in figure 11. From Ambrose and others (2009).

Figure 11. Location of the ETOF, showing distribution of NPA and SPA described in Ambrose and others (2009), Hentz (2010), and Ambrose and Hentz (2010). Core description of Shell No. 55 Watson and ARCO No. B142 wells shown in figures 12 and 15, respectively. Other cored wells, not described in this study, are from Ambrose and others (2014).

Figure 12. (a) Core description of the Shell No. 55 Watson core from 3,600 to 3,734 ft. (b, c) Distal-delta-front facies (interbedded very fine-grained sandstone and silty mudstone. (d, e) Muddy delta-plain facies. (f, g) Fine-grained fluvial interchannel and floodplain facies. Well is located in figure 11.

Figure 13. Gross-sandstone thickness map of the FS1-to-FS2 interval, illustrating a south- and southward-prograding, fluvial-dominated deltaic system in the ETOF.

Figure 32. (a) Phase behavior of ASP composition used in coreflood, (b) cumulative oil recovery and oil cut of ASP flood using Berea Core #40 after equilibrating, and (c) oil cut and cumulative oil recovery of ASP flooding using ETOF Coreflood #4.

TABLES AND FIGURES

Table 1. Original oil in place, estimated ultimate recovery, recovery factor, and remaining oil

Name	OOIP (BSTB)	EUR (BSTB)	RF (%)	Remaining Reserve (BSTB)	Remaining Mobile Oil (BSTB)
Engineering Association, 1993	6.85	5.48	80.0	0.06	0.34
Bureau of Economic Geology, 1982	7.00	5.60	80.0	0.25	0.47
Casey Engineering Inc., 1994	7.03	5.64	80.2	0.25	0.50
W. C. Gussow, 1973	7.50	5.70	76.0	0.61	0.89
Wang, 2010	7.00	5.49*	78.5	0.07*	0.47

* DCA: Decline curve analysis

Table 2. Reservoir parameters of East Texas Oil Field; modified from ETEA (1953)

Discovery Date	September 3, 1930
Counties	Gregg, Rusk, Upshur, Smith, & Cherokee
Acreage (ac)	130,444 (5–10 mi × 45 mi)
Producing Formation	Woodbine
Trap Type	Stratigraphic
Drive Mechanisms	Solution Gas and Water Drive
Top of Formation (ft)	~–3,200 (~3,500)
Dip (degree)	0.5
Original Water–Oil Contact (ft)	–3324.5 ft
Gross Oil Sand Thickness (ft)	51 (max. 125)
Net Oil Sand Thickness (ft)	39
Formation Temperature (F)	146^{o} at –3300 ft subsea
Initial Reservoir Pressure (psia)	1,635
Oil Gravity (API)	39^{o}
Saturation Pressure (psia)	750
Formation Volume Factor (bbl/STB)	1.257
Solution Gas Ratio (scf/STB)	357
Oil Viscosity (cP)	0.983
Formation Water Salinity (ppm)	64,725
Original Oil In Place (BSTB)	6.82–7.03
Well Spacing (ac)	4.2 (0.05–15)
Porosity (%)	25.2
Permeability (mD)	2,098 (1,000–3,000)
Initial Water Saturation (%)	14.1%
Residual Oil Saturation (%)	13.6%

Oil–Water Contact (ft)	–3,324.5
Cumulative Oil (Bbbl)	5.44 as of 10/31/2013
Estimated Ultimate Recovery (Bbbl)	~5.48 by 2030
Daily Oil as of 03/2008 (bbl/d)	10,084
Daily Water Production (Mbbl/d)	11,035
Daily Water Injection (Mbbl/d)	10,094

Table 3. Well statistics, October 2013

Well Type	Number
Producing Wells	3,886
Off-Production Wells	1,764
Plugged Wells	24,162
Dry Holes	768
Total	30,580

Table 4. Summary of workover and deepening/recompletion tests

Well Name	Production in 08/10		Completion Date	Type of Operation	Perforation Interval	Stringer	Oil Rate	Water Rate	Cost	Estimated Oil Production (STB)	EUR	Comment
	Oil (bbl/d)	Water (bwpd)			ft		bbl/d	Bwpd		As of June 2014	STB	
Recompletion												
Akin, J. W. #1	0	505	08/01/10	Deepening	3644-56, 3667-71	S2	0		$95,000			Problems to separate main and lower stringer
Akin, J. W. #10	1	466	03/01/11	Deepening	3623-3640	S2	39		$92,000	22,393	25,000	
Akin "B" #15	0	366	06/01/11	Deepening	3600-3634	S2			$101,000			
Bassham 8	0.3	347	10/05/12	Deepening		S2	70			21,000	35,000	
Moncrief 38	5	432	02/01/11	Recompletion	3620-30	S2			$35,000	27,720	35,000	S1 will be tested next
Boston Moore -B- #17			09/23/12	Deepening	3570-84	S2	15			4,500	10,000	
Moncrief 13	0	305	10/10/12	Deepening		S2						Casing collapse
Moncrief 22	2.5	456	07/01/11	Deepening		S2	40		$135,000	17,730	25,000	
Moncrief 28	1.5	351	03/11/11	Deepening		S2	0		$73,000			To open up additional opportunities
Moncrief 53			10/10/12	Deepening		S2						Mechanical failure
Turner, M. #15	1	450	05/15/11	Deepening	3611-42	S2	13		$105,000			
Subtotal									**$636,000**	**93,343**	**130,000**	
Workover												
Boston Moore "A" #1	1.1	263	08/01/10	Cleaning & reperforation	3584-94	S2	10	108	$24,000	6,903	10,000	
Boston Moore "B" #9	13	83	12/01/10	Pump repair		S2	50	70	$8,500	22,617	30,000	
Boston Moore "B" #14	15	74	06/29/12	Reperforation		S2	30	147		24,058	40,000	
Turner, M. #16	0.3	396		Recompletion		Main	0		$84,000			Not deep enough and missed 20-30 ft
Subtotal									**$116,500**	**53,577**	**80,000**	
Total									**$752,500**	**146,919**	**210,000**	
Other												
Boston Moore "B" #2	1.4	5.8	08/18/10			S2	31	52		14,376	20,000	
Boston Moore "B" #10	16.5	139	11/16/10			S2	36	168		24,300	50,000	
Subtotal										38,676	70,000	

Table 5. Properties of Berea sandstone core

Berea Core Sample	Pore Volume (cc)	Porosity	K (md)
Test #1	5.82	0.21	96.9
Test #2	5.32	0.19	142.0
Test #3	4.99	0.17	294.2

Table 6. Properties of ETOF reservoir core

ETOF Core Sample	Pore Volume (cc)	Porosity	K (md)
Test #1	5.86	0.17	77.9
Test #2	4.82	0.14	26.9
Test #3	6.90	0.22	10.8
Test #4	5.70	0.17	48.9

Table 7. Core flow test results of Berea sandstone

System Pressure	Swr	Sor	Sorco2	Swrco2	SCO2	Oil Recovery of ROIP (%)
1945 psi	0.16	0.49	0.05	0.49	0.46	90.11
1748 psi	0.12	0.43	0.07	0.43	0.50	83.33
1410 psi	0.28	0.35	0.17	0.41	0.42	52.02

Table 8. Core flow test results of ETOF core

System Pressure	Swr	Sor	Sorco2	Swrco2	SCO2	Oil Recovery of ROIP(%)
1994psi	0.37	0.50	0.15	0.48	0.37	69.97
1763psi	0.22	0.58	0.18	0.40	0.42	68.35
1386 psi	0.29	0.58	0.35	0.40	0.25	39.70
1122 psi	0.26	0.58	0.44	0.40	0.16	24.24

Table 9. Summary of chemical floods parameters and results

Run #	1	2	3	4	5	6	7
Rock sample	Berea, 1ft. long	Berea plug 1	Berea plug 2	ETOF-9	ETOF-8	Berea plug 3	ETOF-6
Formulation	H	H	H	H	I	M*	O
Surfactants*	S13D/S2	S13D/S2	S13D/S2	S13D/S2	S13D/S2/ Cedepal	S13D/ TDA12/ Cedepal	S13D/ TDA12/ Cedepal
Surf. conc.(wt%)	0.3/0.2	0.3/0.2/1	0.3/0.2/1	0.3/0.2	0.33/0.17/ 0.09	0.5/0.25/ 0.25	0.34/0.5/ 0.16
Alcohol* Conc.(w%)	SBA 1.0	SBA 1.0	SBA 1.0	SBA 1.0	SBA 0.5	-	-
Polymer* Concent.	F3330s 2500ppm	F3330s 2500ppm	F3330s 2500ppm	F3330s 2500ppm	3330s 2500ppm	F3530s 2000ppm	F3530s 2200ppm
Salt	3.53% NaCl	3.53% NaCl	3.65% NaCl	3.65% NaCl	5.3% NaCl	SSFB**	SSFB**
Brine in core	3.53% NaCl	3.53% NaCl	3.53% NaCl	SSFB**	SSFB**	SSFB**	SSFB**
Drive polymer conc./salinity(ppm/%)	2750 2.75%	2750 2.75%	2750 2.8%	2750 2.8%	2750 4.2%	2000/ 50% SSFB**	2000/ 70% SSFB**
Slug volume (PV)	0.6	0.6	0.6	0.6	0.6	0.6	0.6
Oil breakthrough (PVI)	0.22	0.35	0.3	0.3	0.5	0.45	0.5
Maximum Oil cut (%)	50	57	29	12.5	13.5	37	12
Final oil saturation	0.034	0.143	0.022	0.23	0.197	0.045	0.181
Tertiary Oil Recovery (%)	91	72	93	28	32	86	24
Chemical consumption (lb of surf+alc+pol /bbl of oil	10.6	10	14.9	41	30.9	9.5	44.9

*CF406A = Cedepal FA-406; S13D = PetroStep 13D; S2 = Petrostep S2; SBA= sec butyl alcohol; F3530S and F3330s are Flopaam series polyacrylamides from SNF.
**SSFB = Aq. solution of: 5.86 w%NaCl + 0.5 w%CaCl2.2H2O + 0.45 w%MgCl2.6H2O; 6.45% TDS.

Figures

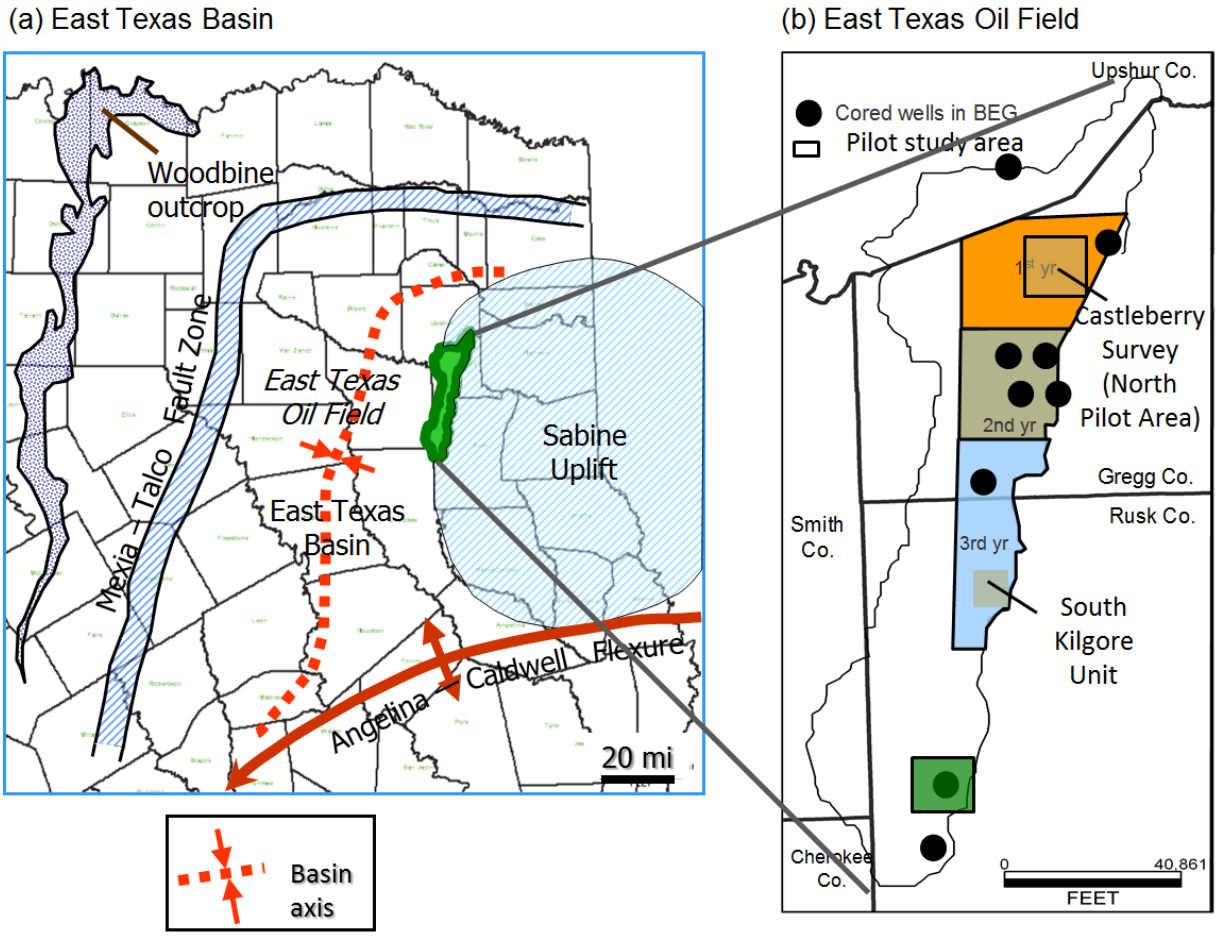

Figure 1. (a) Location map of East Texas Basin showing East Texas Oil Field (ETOF) field outline; (b) Outline of field showing three study phases and core locations used in mapping the depositional trends of lower Woodbine (“stringer”) sandstones.

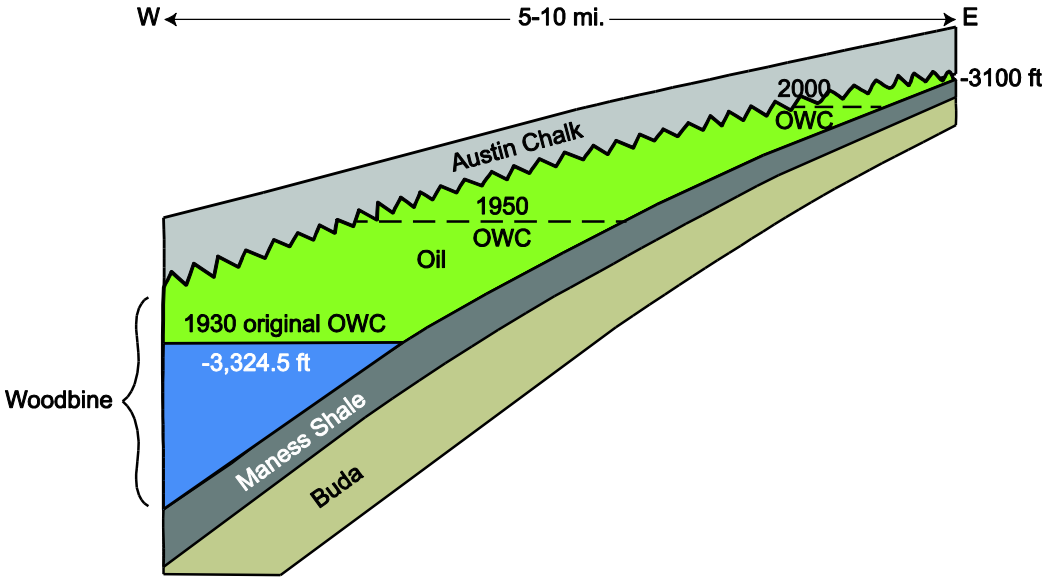

Figure 2. Schematic diagram showing formations and wedge-type geometry of Woodbine Reservoir in the ETOF.

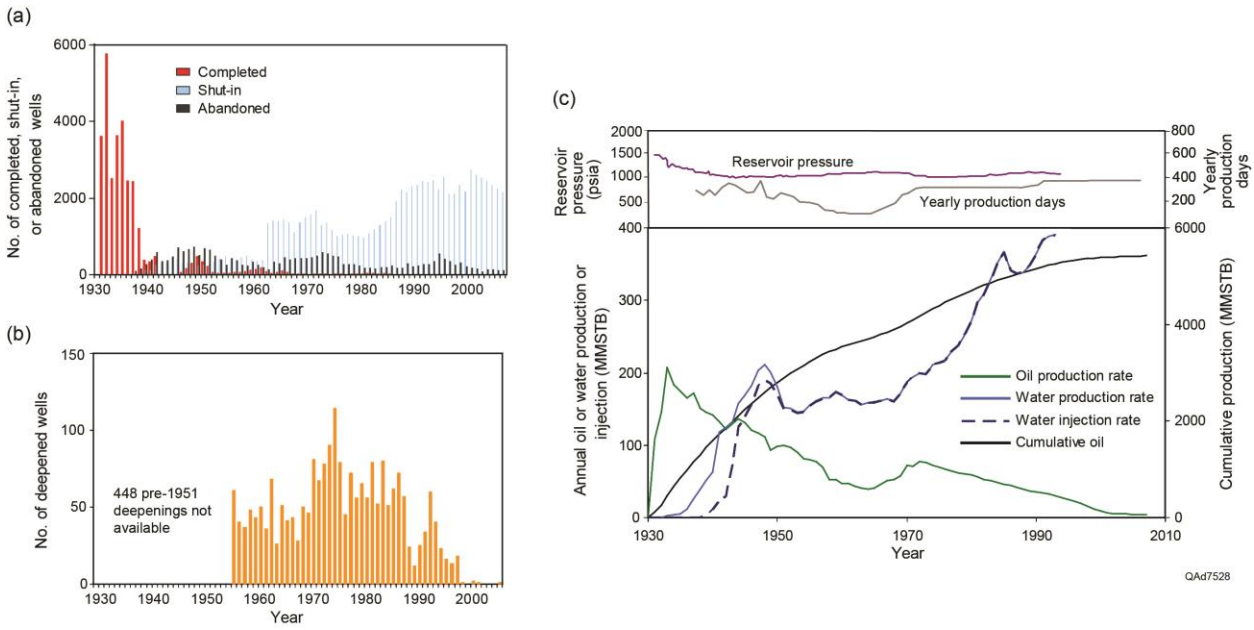

Figure 3. Statistics of (a) completion, shut-in, and abandoned wells; (b) a deepened wells; and (c) pressure and production history. Data from ETEA and Casey Engineering (1994).

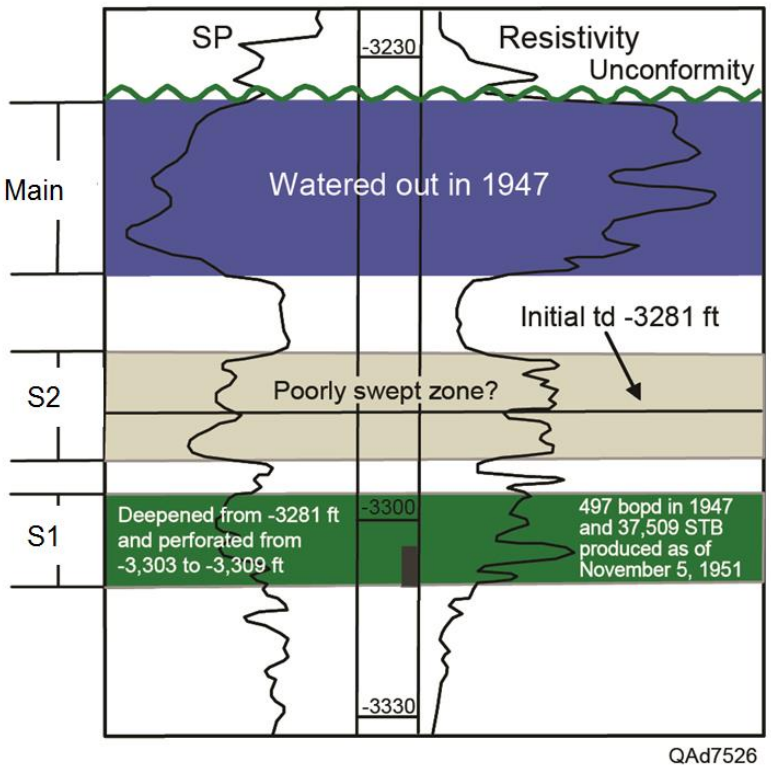

Figure 4. Example of deepening/recompletion in S1 stringer in 1947.

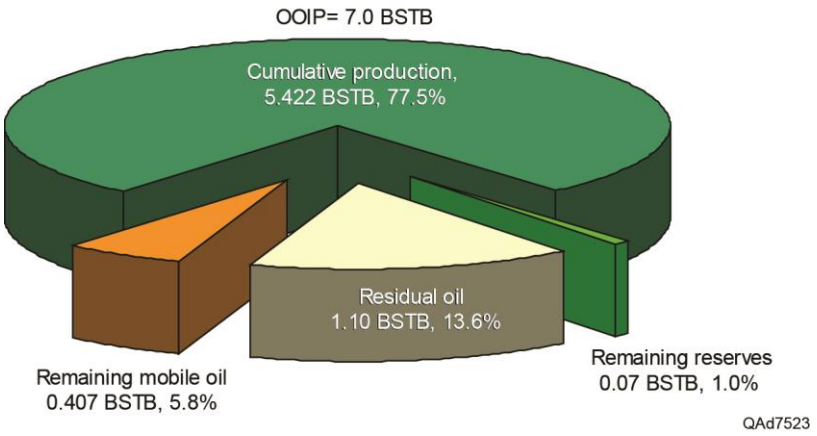

Figure 5. Cumulative production, remaining mobile oil, remaining reserve, and residual oil distribution.

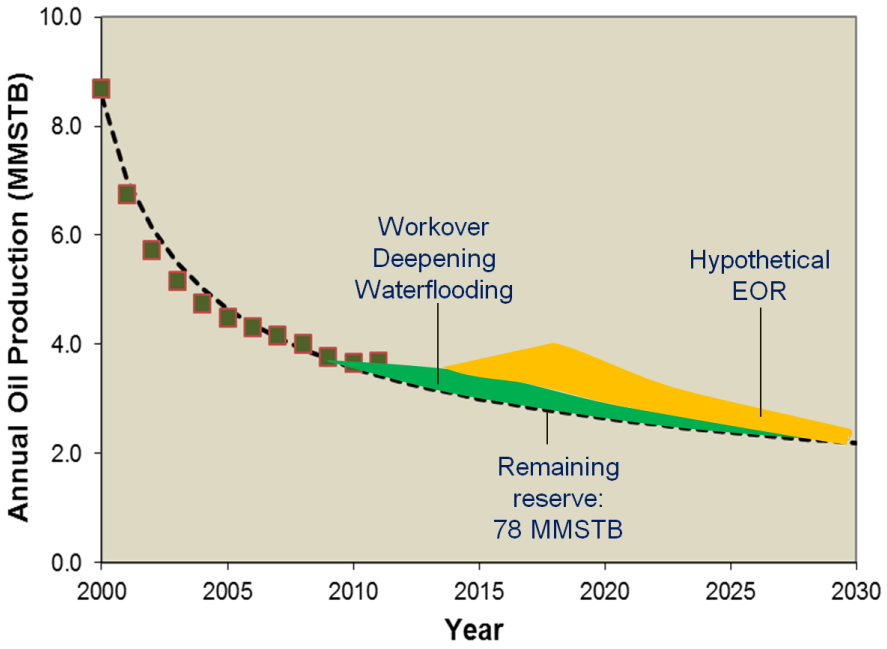

Figure 6. Effects of workover, deepening/recompletion, miniwaterfloods, and EOR on ETOF future production.

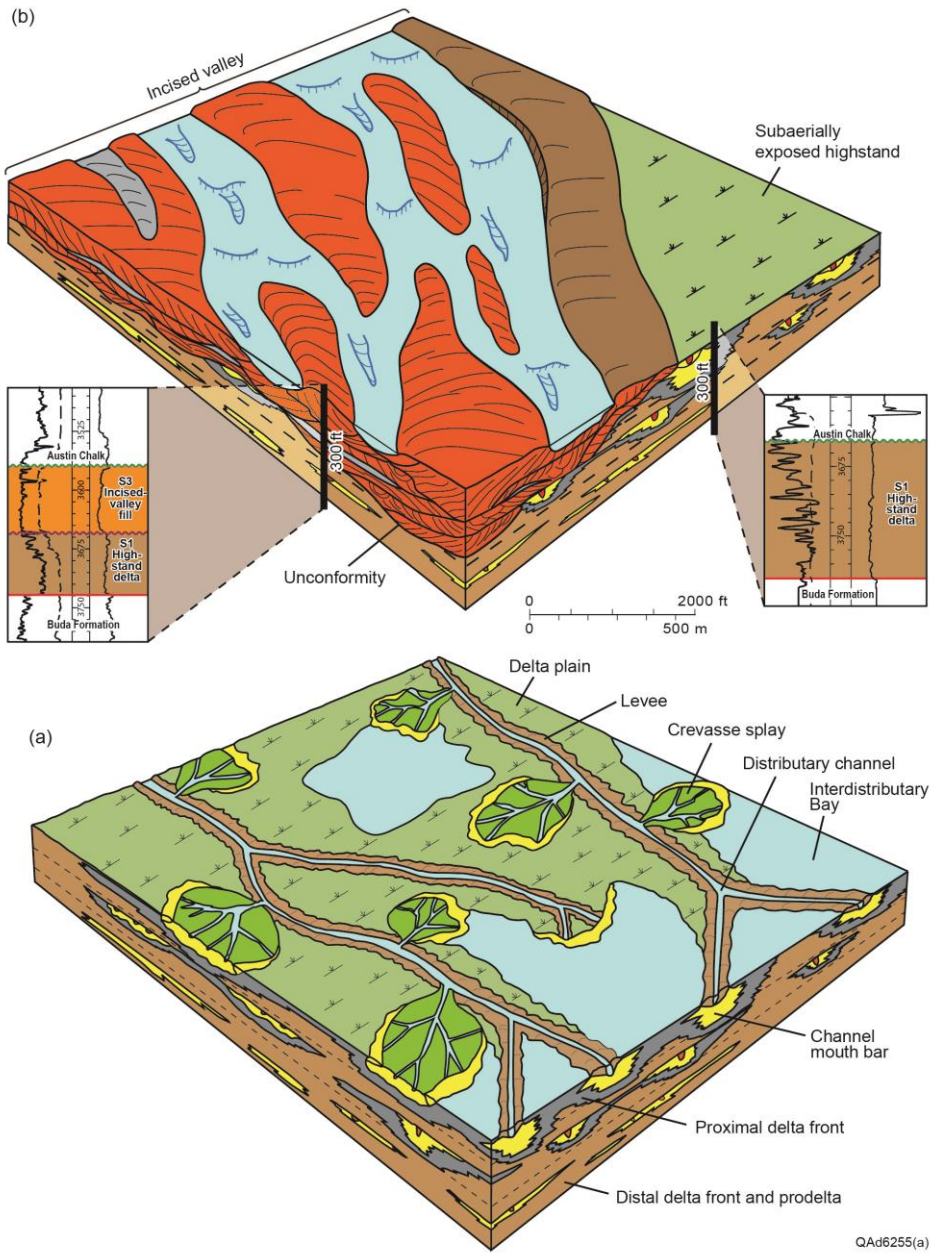

Figure 7. Stratigraphic architecture in the Woodbine Group of the ETOF. (a) Highstand fluvial-dominated deltaic deposits (“stringer sands”). (b) Lowstand incised-valley fill deposits (“main sand”) truncating lower section of deltaic deposits. Modified from Ambrose and others (2009) and Ambrose and Hentz (2010).

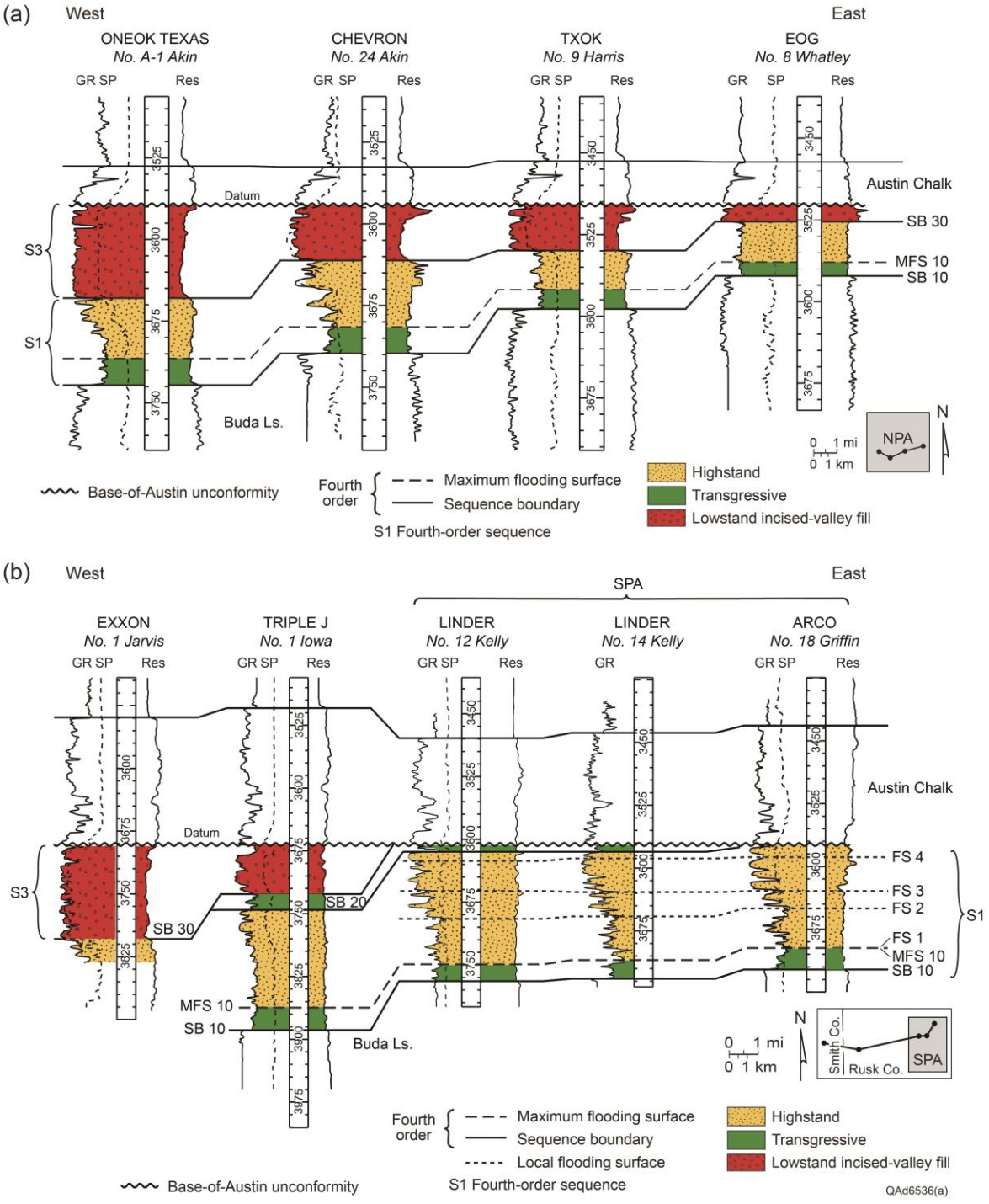

Figure 8. (a) Representative structural-dip cross section of the North Pilot Area (NPA), showing inferred fourth-order sequence stratigraphic surfaces and systems tracts. The datum is the base-of-Austin unconformity. No horizontal scale. (b) Representative structural-dip cross section of the South Pilot Area (SPA), showing inferred fourth-order sequence-stratigraphic surfaces and systems tracts. The datum is the base-of-Austin unconformity. No horizontal scale. GR = gamma ray; SP = spontaneous potential; Res = resistivity; SB = sequence boundary.

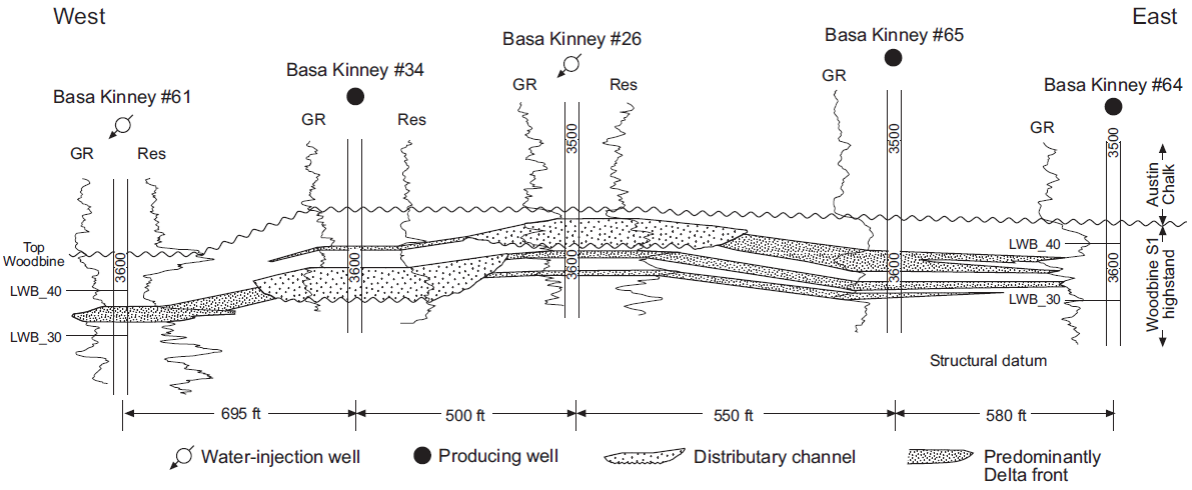

Figure 9. West–east structural cross section in the Kinney Lease in the SPA, showing location of producing and water-injection wells and complex deltaic facies architecture in the lower Woodbine (LWB) 30–40 interval (FS3 to FS4, this study) in the highstand deltaic succession. GR = gamma ray; Res = resistivity. Line of section is shown in figure WAA 10a. Location of SPA shown in figure 11. From Ambrose and others (2009).

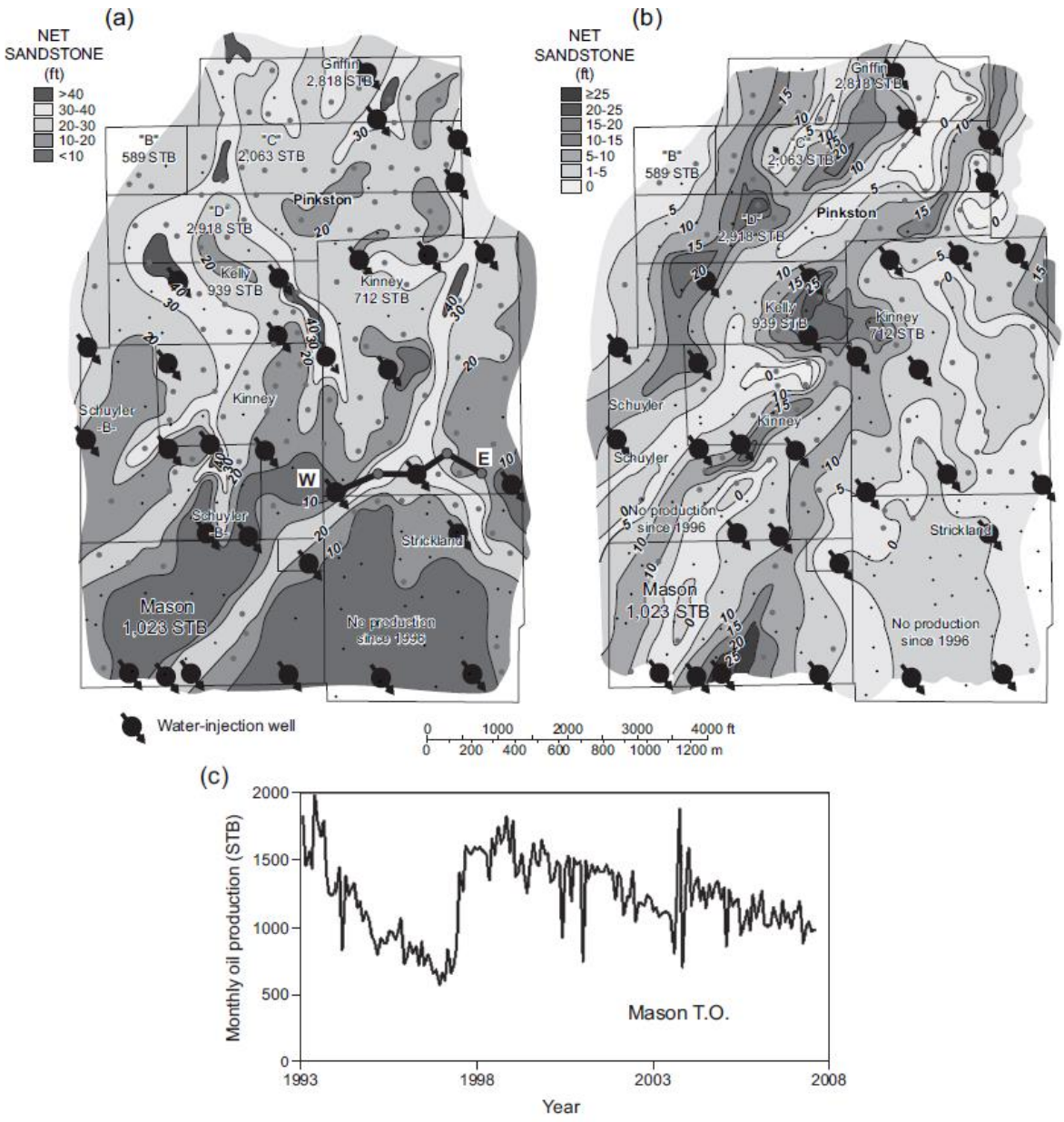

Figure 10. Sandstone thickness maps of two highstand deltaic stringer sandstone depositional units in the SPA in the southern part of the ETOF. (a) Net sandstone in the LWB 30–40 unit (FS3 to FS4, this study). (b) Net sandstone in the LWB 20–30 unit (FS2 to FS3, this study). LWB 20–30 and LWB 30–40 nomenclature is defined in Ambrose and others, 2009). (c) Monthly oil production in stock tank barrels (STB) from the Mason Lease from 1993 to 2007. Increased oil production in the Mason Lease (southwest corner of maps) in 1997 resulted from water injection into transmissive, southwest-trending distributary-channel sandstones in the LWB 30–40 unit. West–east structural cross section in the Kinney Lease is shown in figure 9. Location of SPA is shown in figure 11. From Ambrose and others (2009).

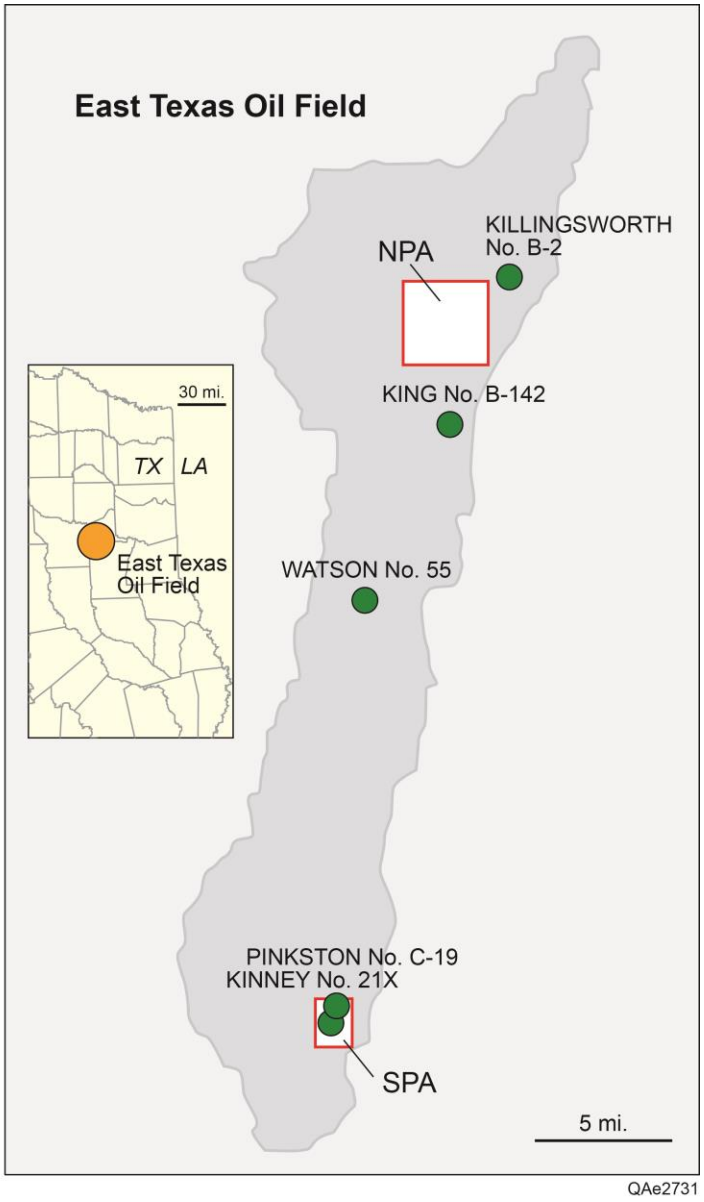

Figure 11. Location of the ETOF, showing distribution of NPA and SPA pilot areas described in Ambrose and others (2009), Hentz (2010), and Ambrose and Hentz (2010). Core description of Shell No. 55 Watson and ARCO No. B142 wells shown in figures 12 and 15, respectively. Other cored wells, not described in this study, are from Ambrose and others (2014).

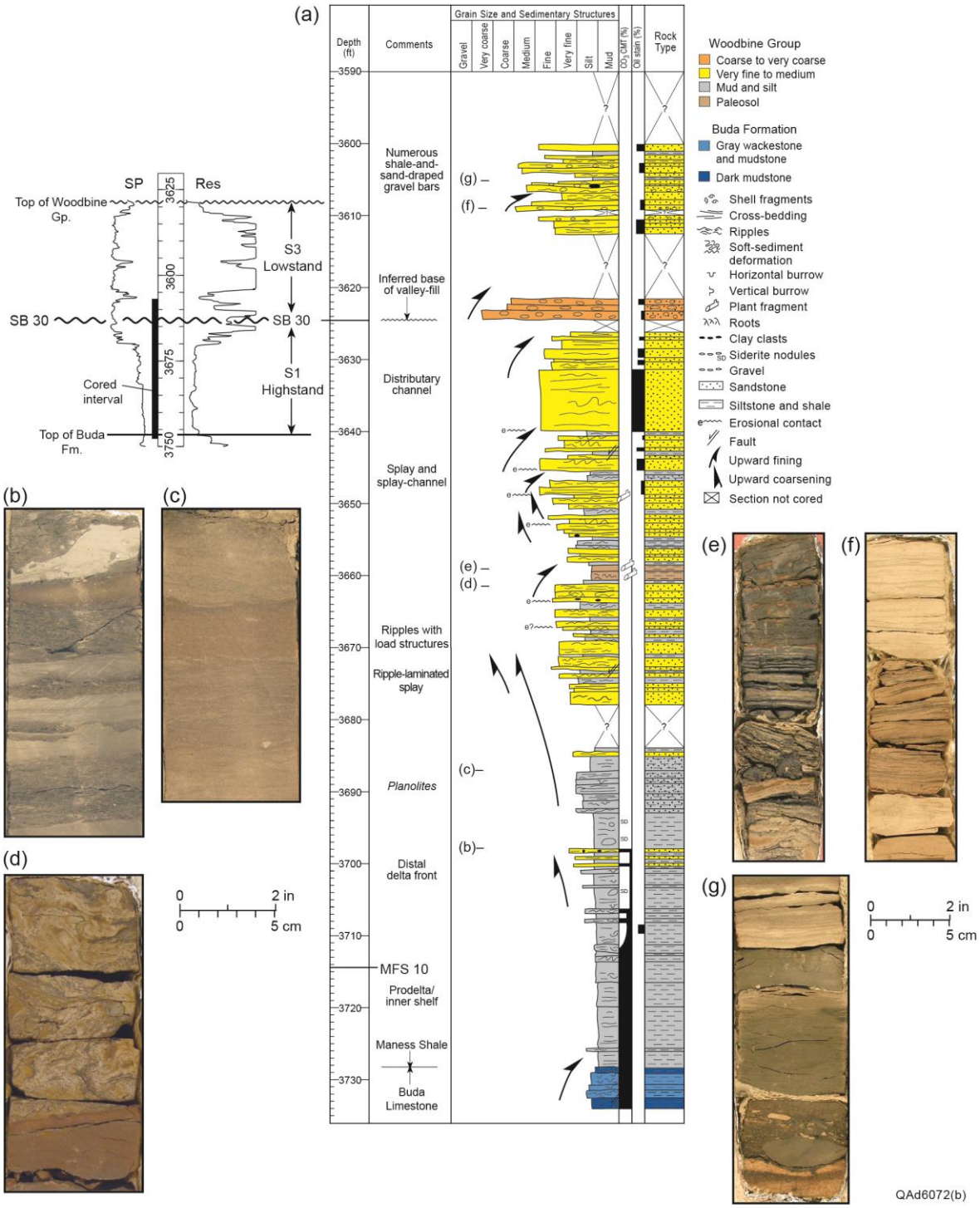

Figure 12. (a) Core description of the Shell No. 55 Watson core from 3,600 to 3,734 ft. (b, c) Distal-delta-front facies (interbedded very fine-grained sandstone and silty mudstone. (d, e) Muddy delta-plain facies. (f, g) Fine-grained fluvial interchannel and floodplain facies. Well is located in figure 11.

See PDF attachment - Figure13-QAe2835

Figure 13. Gross-sandstone thickness map of the FS1-to-FS2 interval, illustrating a south- and southward-prograding, fluvial-dominated deltaic system in the ETOF.

See PDF attachment - Figure14-QAe2833

Figure 14. Gross-sandstone thickness map of the FS2-to-FS3 interval, illustrating a south- and southward-prograding, fluvial-dominated deltaic system in the ETOF.

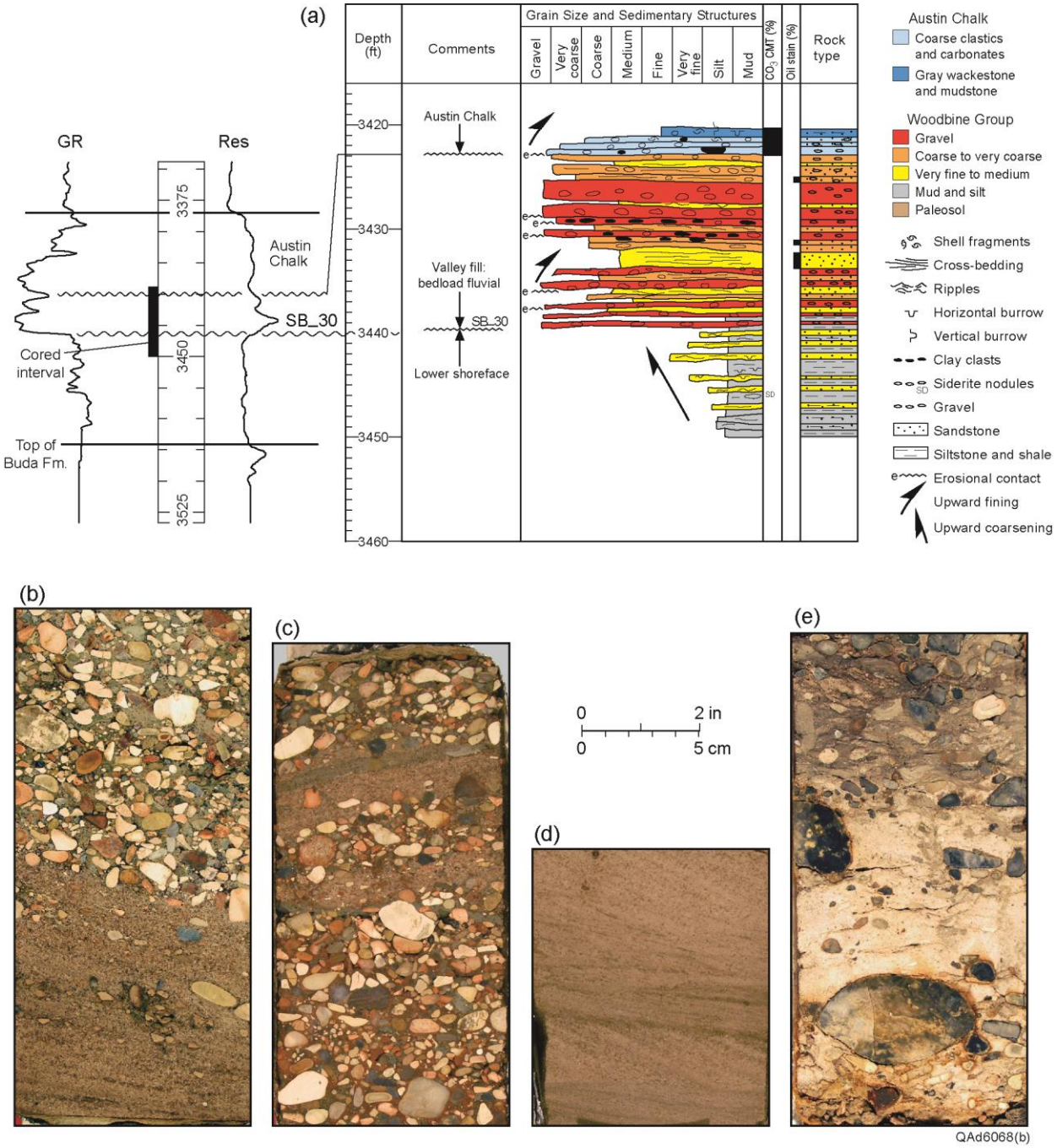

Figure 15. (a) Core description of the ARCO No. B142 King core from 3,420 to 3,450 ft. (b, c) Chert-pebble conglomerate interbedded with very coarse-grained sandstone at 3,437.4 and 3,438.6 ft, respectively. (d) Crossbedded, coarse-grained sandstone at 3,437 ft. (e) Unconformity at base of Austin Chalk at 3,423 ft. Well is located in figure 11.

See PDF attachment - Figure16-QAe2834

Figure 16. Gross-sandstone thickness map of the lowstand incised-valley system in the ETOF. Eastward-thinning thickness values reflect increasing truncation by the base-of-Austin-Chalk unconformity.

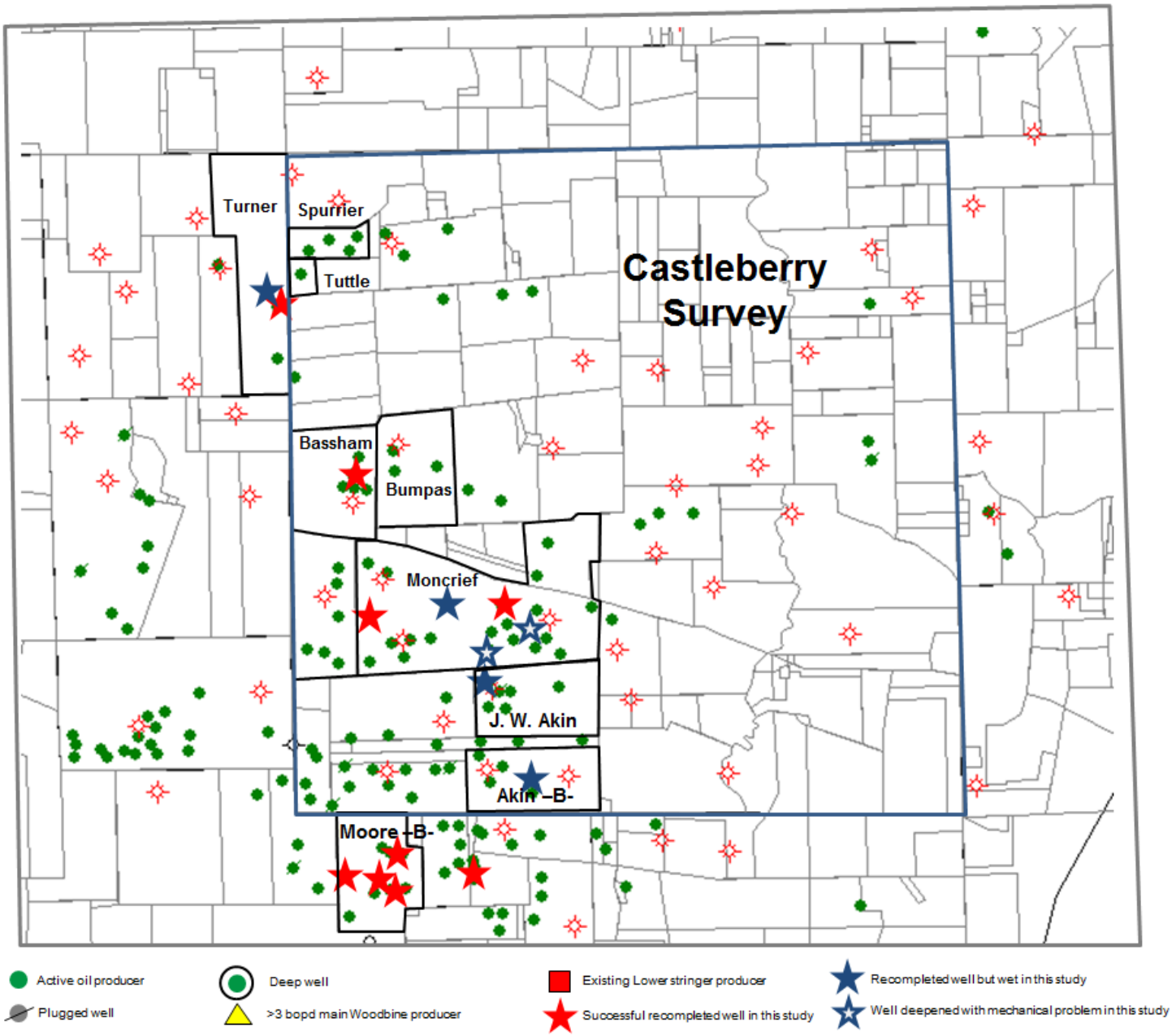

Figure 17. Lease and wells used for selecting workover and deepening targets. Solid asterisks are successful wells and open asterisks are unsuccessful wells.

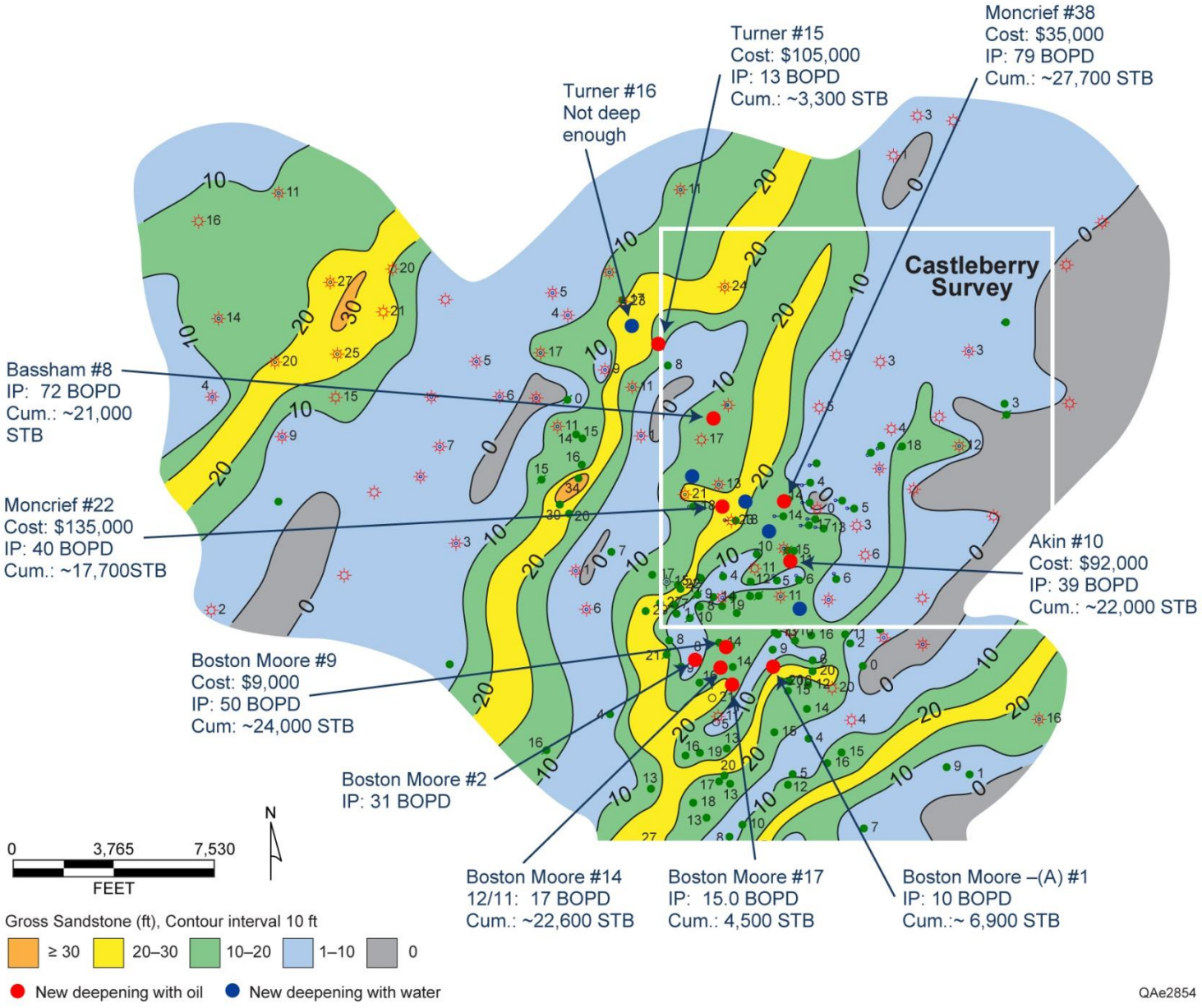

Figure 18. Summary of workover and deepening tests, S1 and S2 stringer sands.

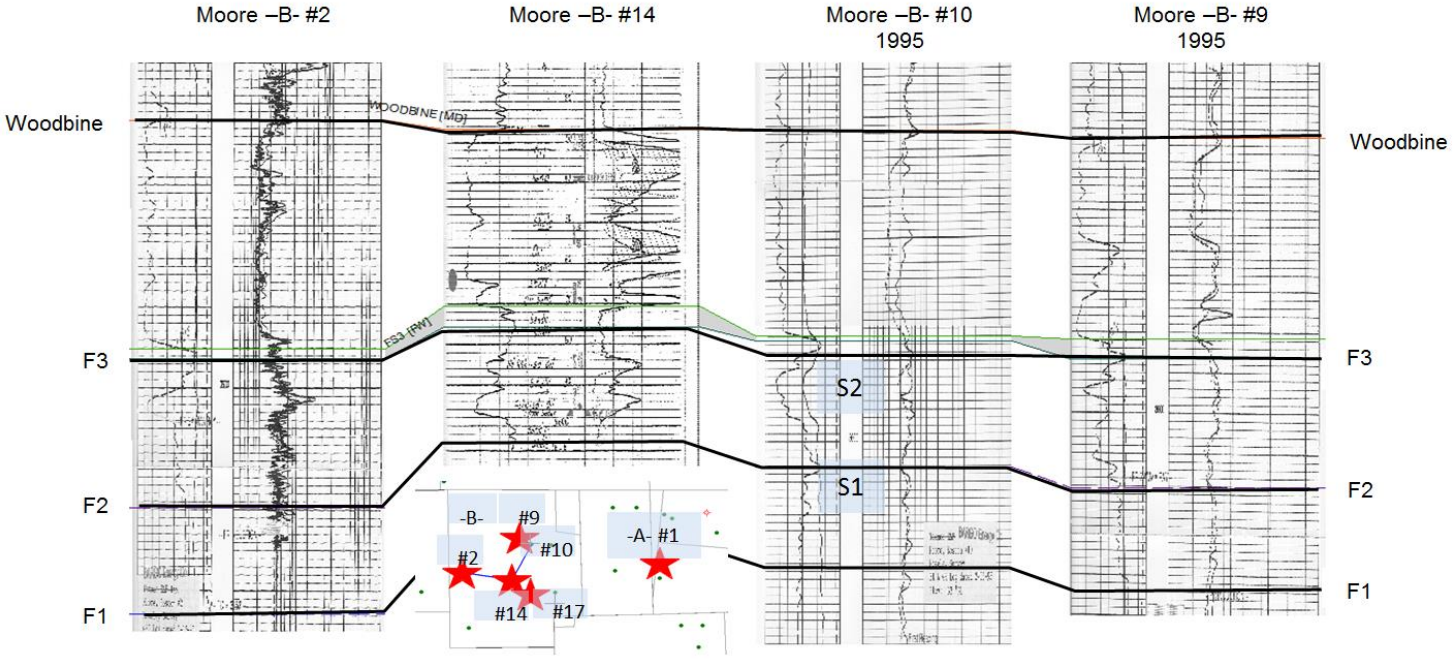

Figure 19. Cross section showing S1 and S2 lower stringers in Boston Moore “B” lease.

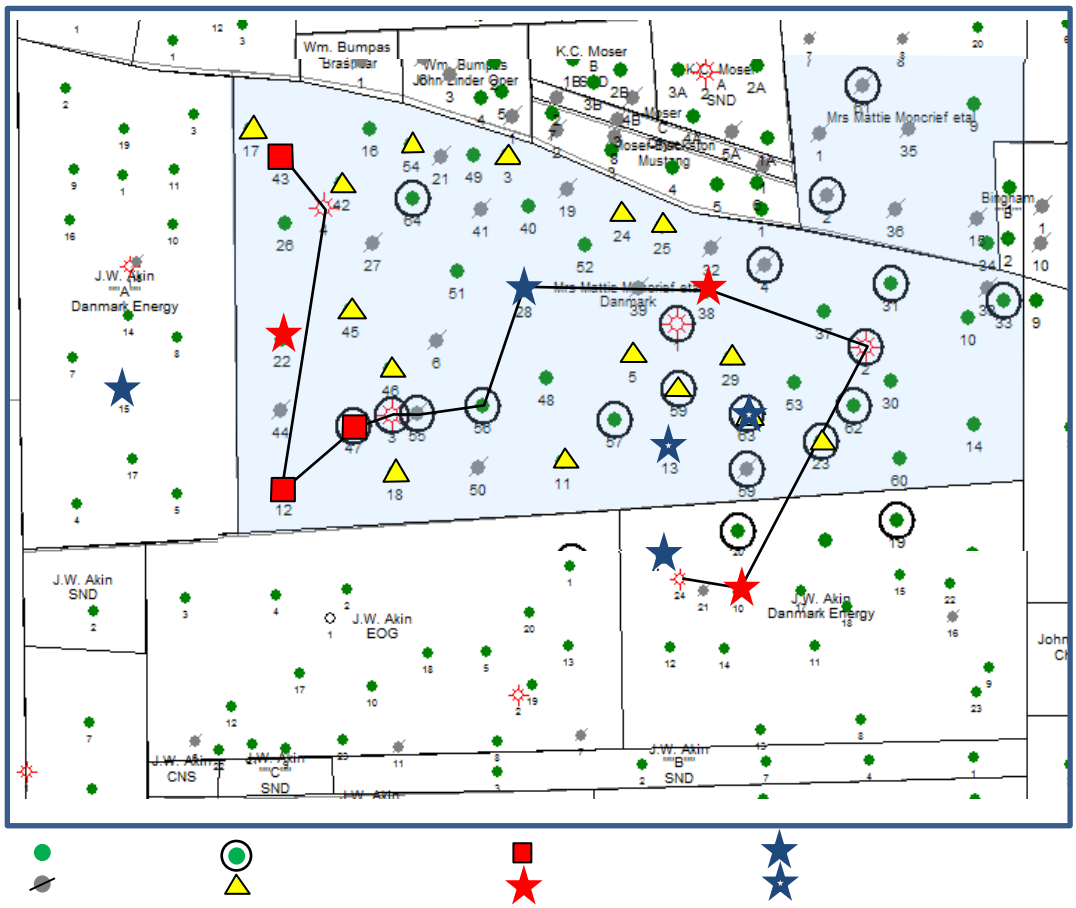

Figure 20. Basemap showing well status in Matt Moncrief Lease.

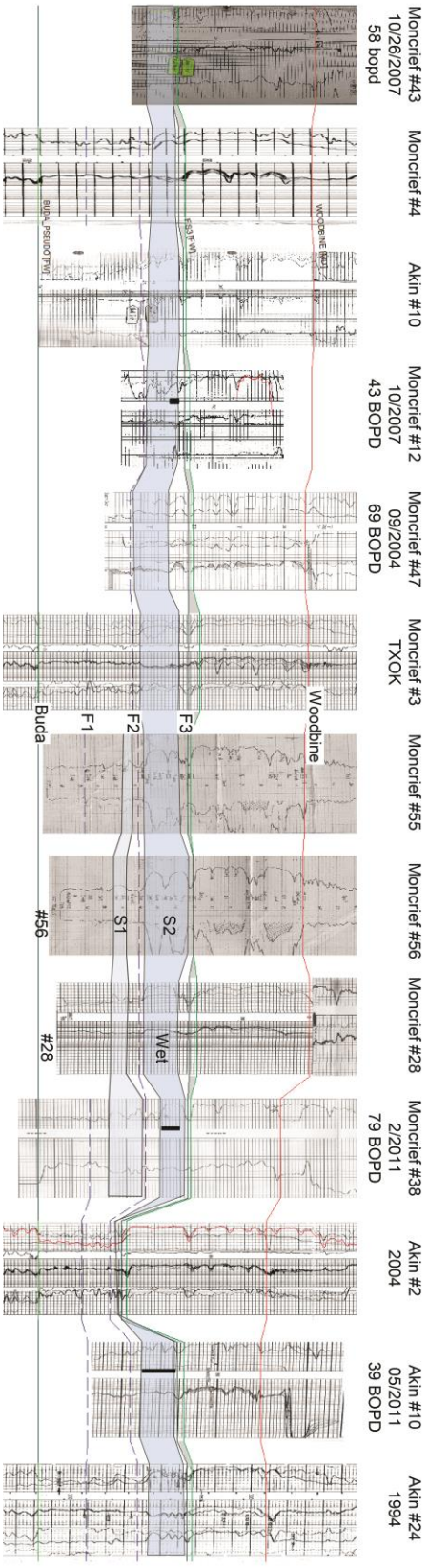

Figure 21. W–E cross section showing S1 and S2 stringer sandstones in Matt Moncrief and J. W. Akin Leases, and deepening intervals and results.

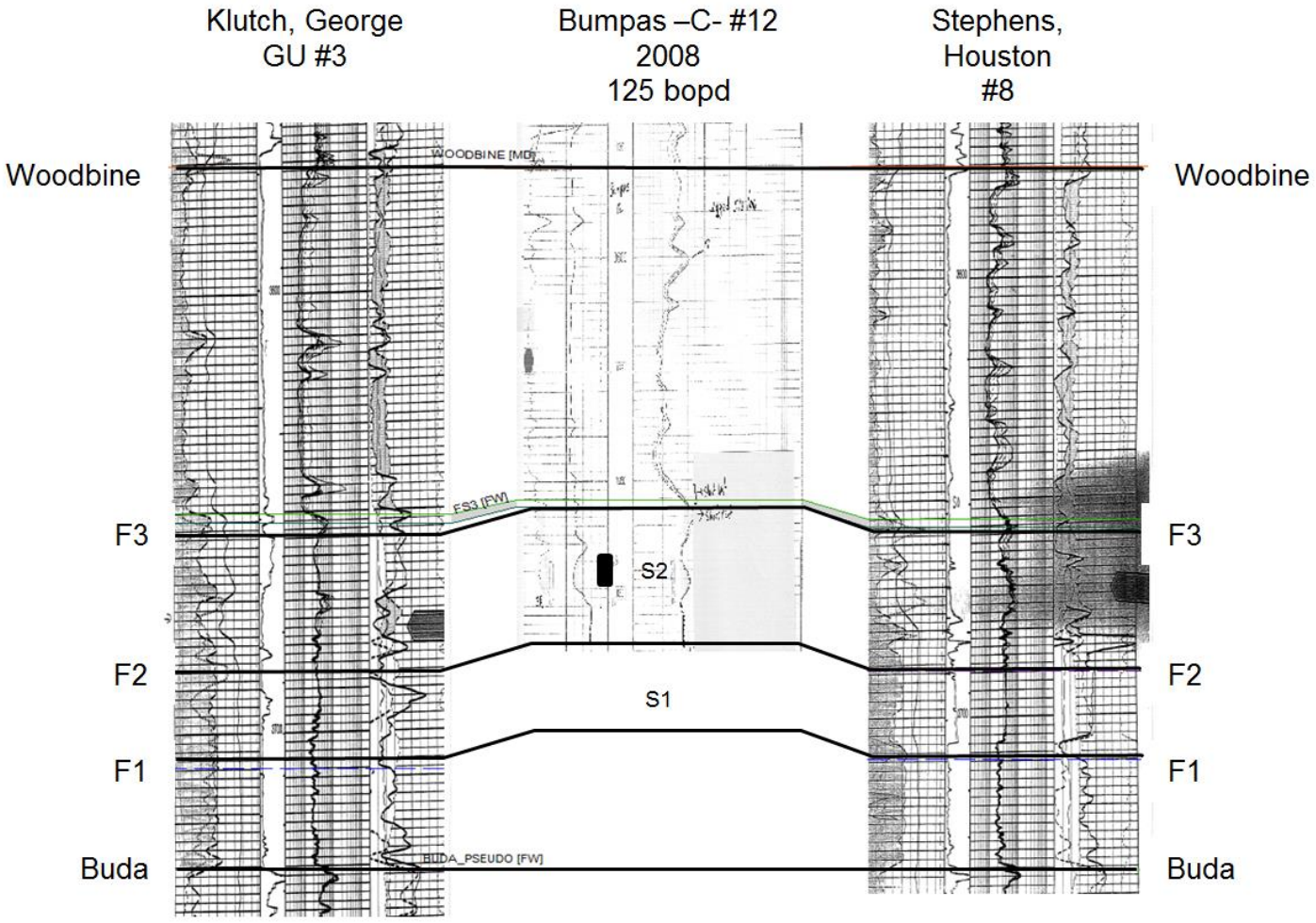

Figure 22. SW–NE cross section in Bumpas-Bassham area showing S2 stringer sandstone. The Bumpas “C” #12 was recompleted with an initial rate of 125 bbl/d in 2007.

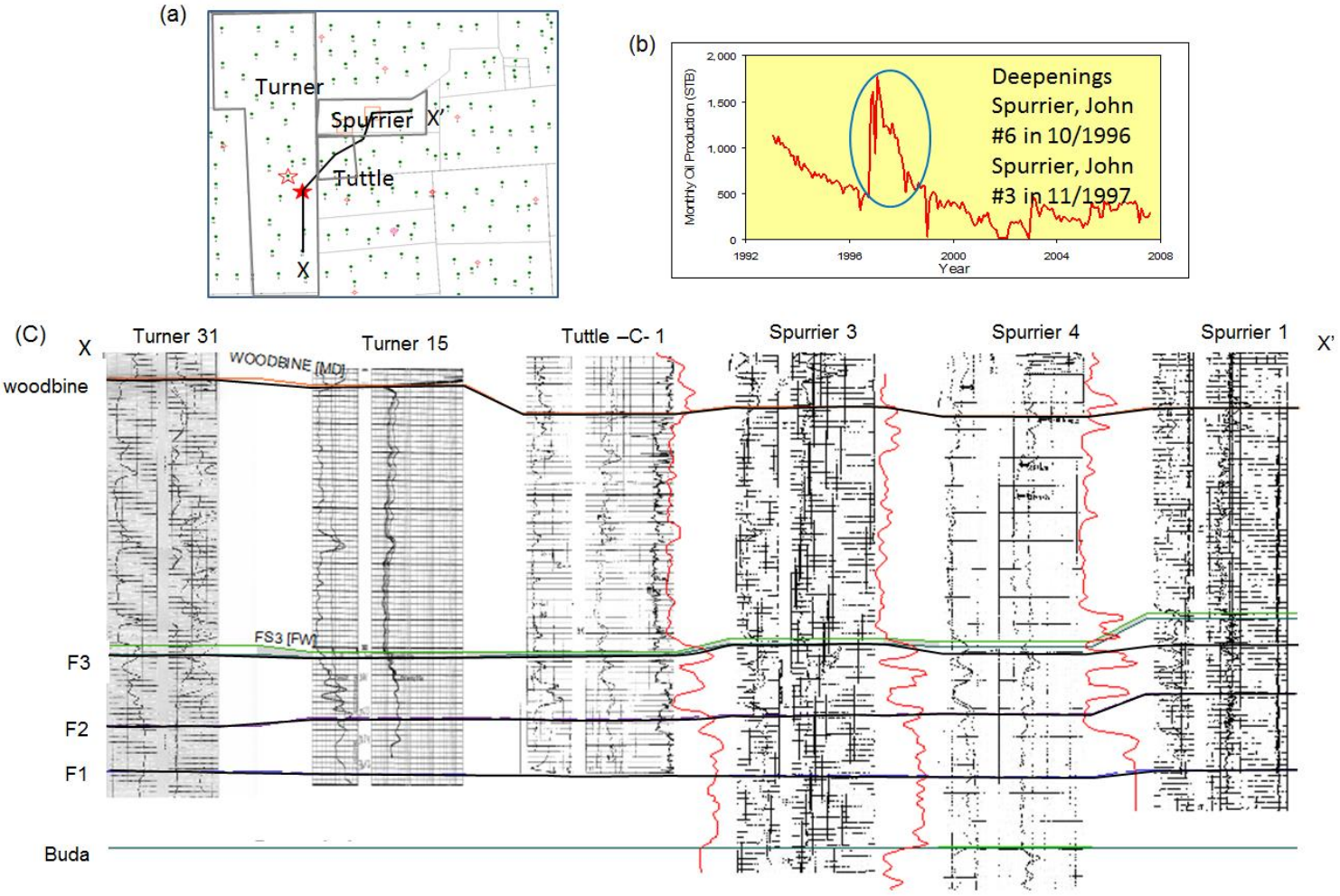

Figure 23. (a) Basemap, (b) monthly lease production, and (c) cross section in Turner-Spurrier Leases.

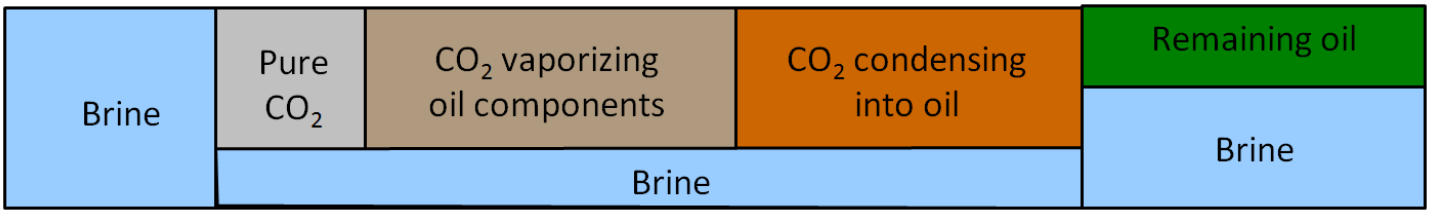

Figure 24. Mechanisms of CO_2 flooding.

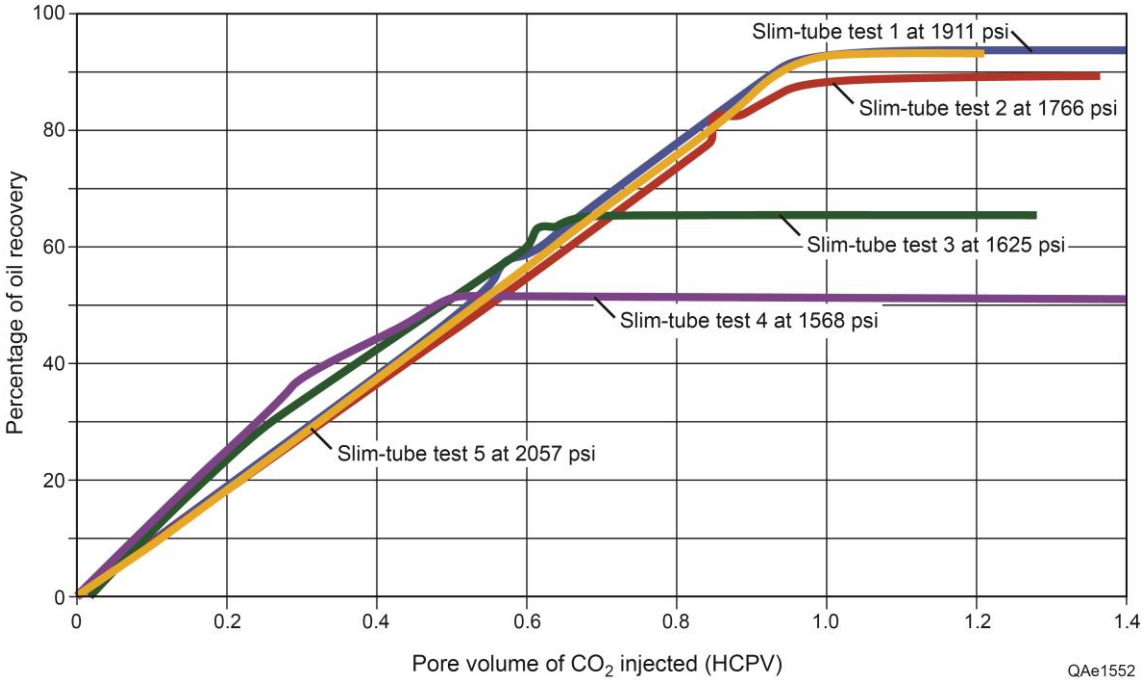

Figure 25. Production history of slim-tube experiment at different pressures.

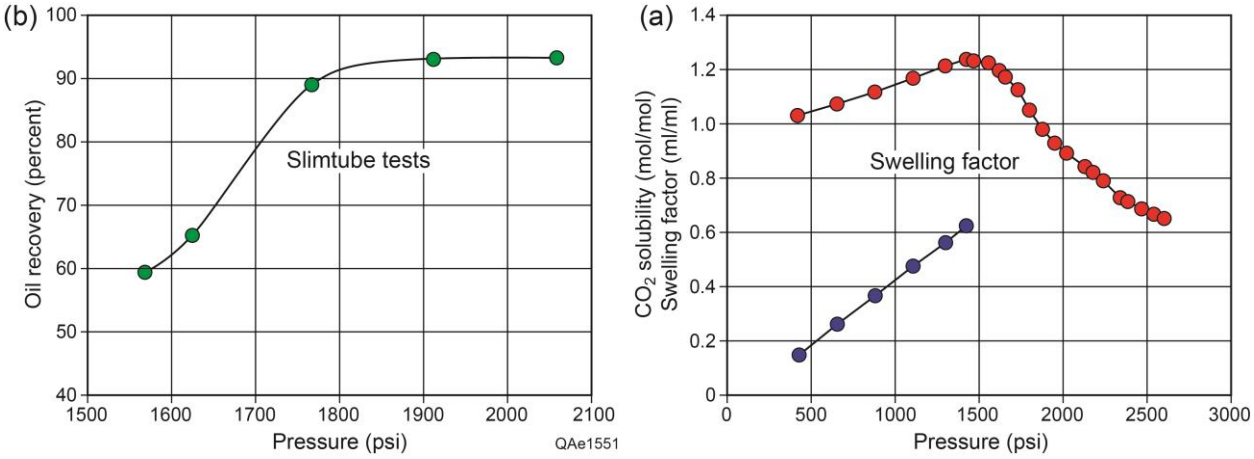

Figure 26. (b) Swelling/extraction curve of ETOF crude oil with carbon dioxide at 146°F and (a) MMP defined from slim-tube experiment.

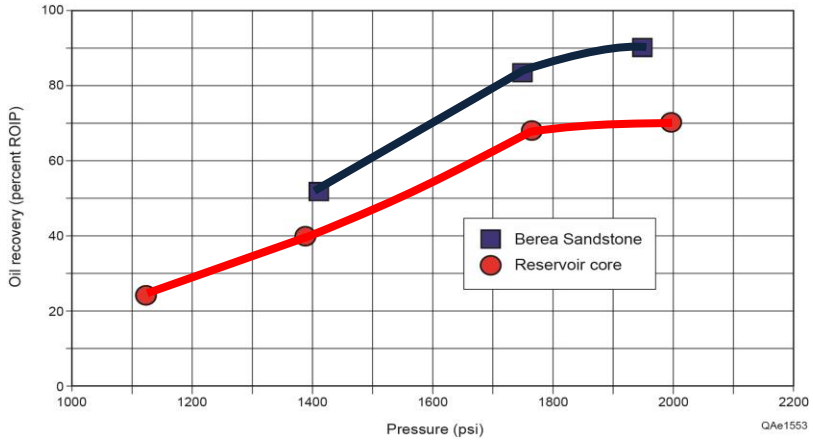

Figure 27. Tertiary oil recovery by CO_2 injection at 146°F.

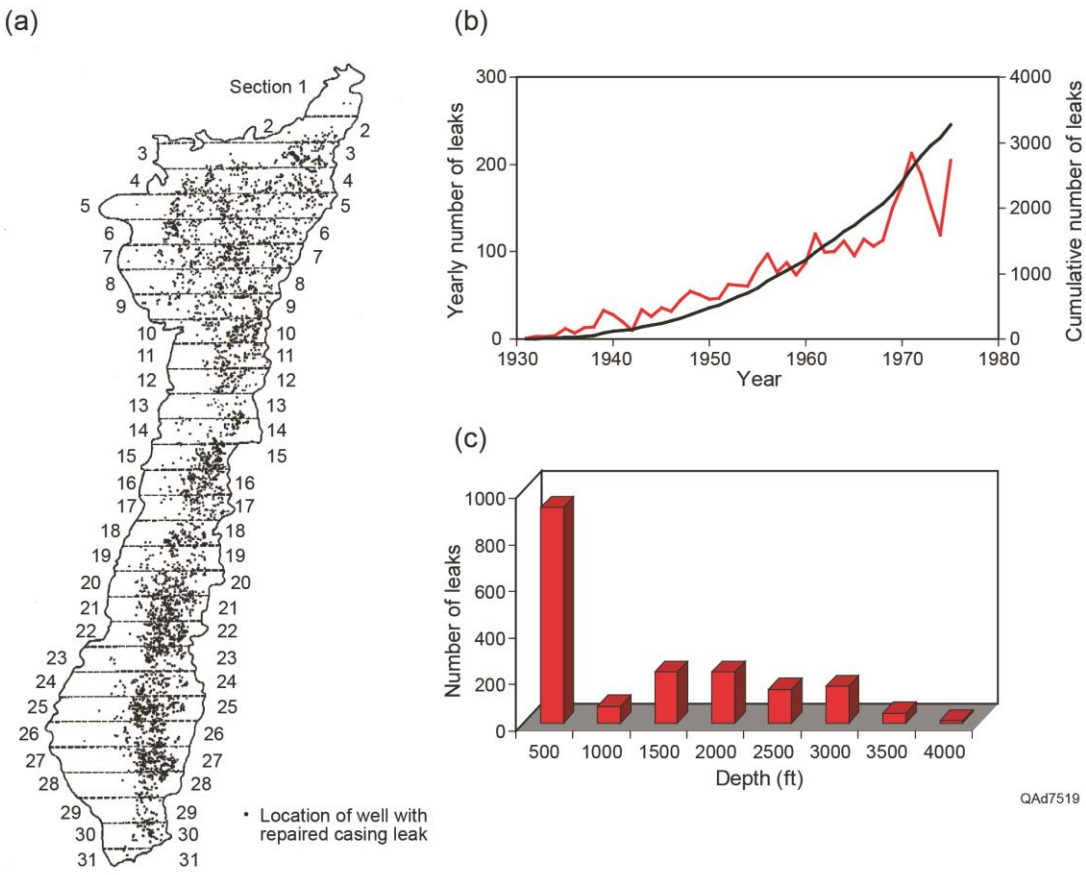

Figure 28. Statistics of casing leaks in the ETOF (from ETEA, 1972).

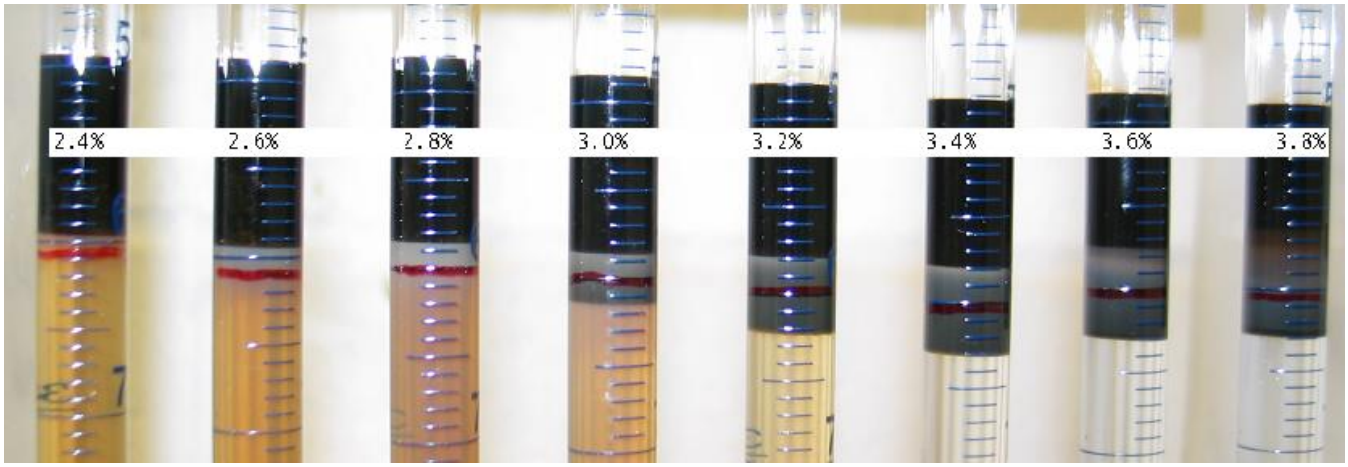

Figure 29. Salinity scan (NaCl %) for the formulation A in table 2 @ 63°C.

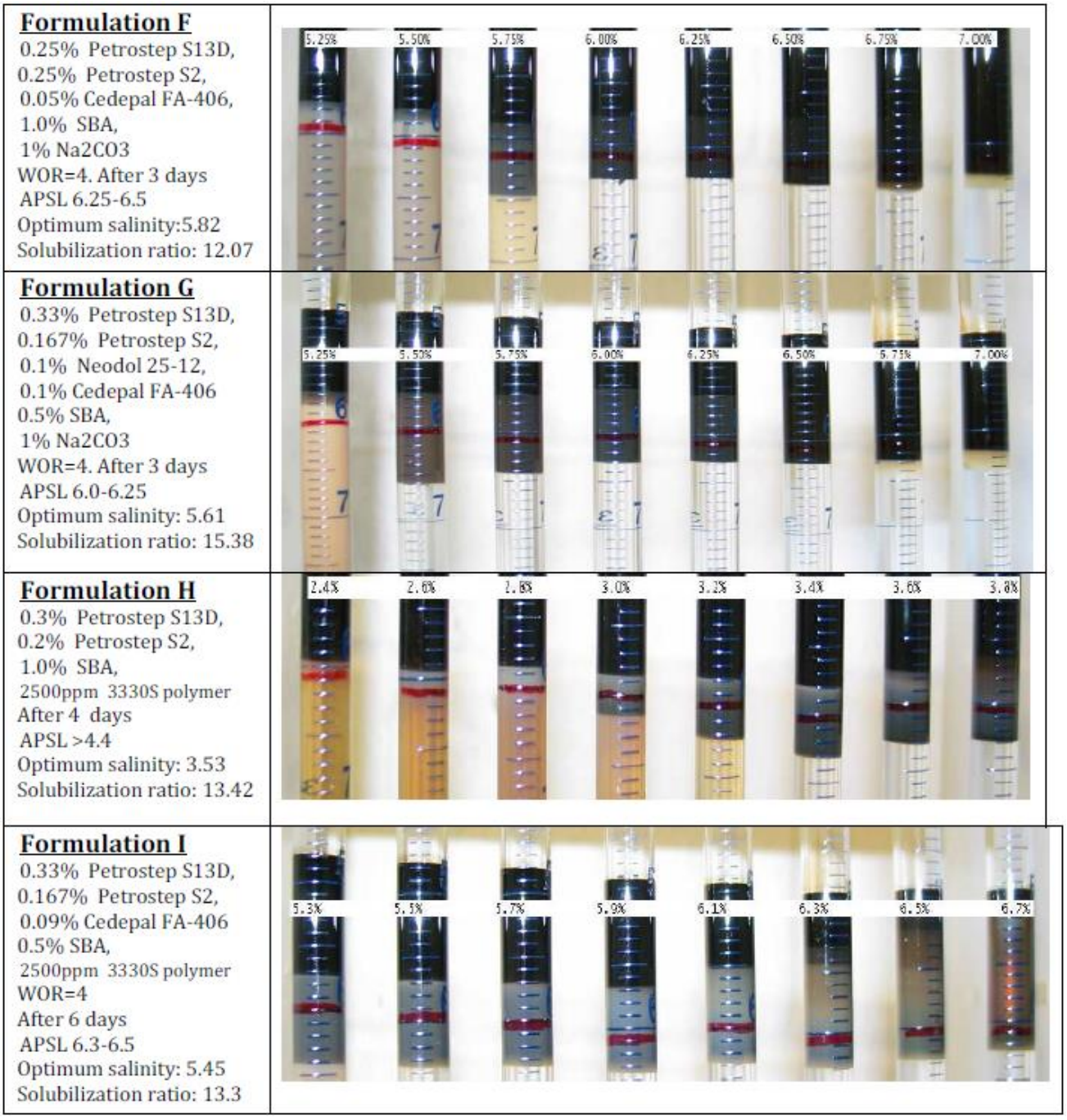

Figure 30. Phase behavior for four different formulations with 0.5% surfactant concentration.

	**ETOF-0** **Well:** Shell Watson 55 **Depth:** 3631' **Length:** 3.56 cm **Diameter:** 3.76cm **Notes:** Too short, broken end.		**ETOF-1** **Well:** K. Lawson #1 **Depth:** 3774.4' **Length:** 5.64 cm **Diameter:** 3.77 cm **Notes:** Almost impermeable
	**ETOF-2** **Well:** K. Lawson #1 **Depth:** 3778.5' **Length:** 5.46 cm **Diameter:** 3.78 **Notes:** black streak embedded. Almost impermeable		**ETOF-3** **Well:** K. Lawson #1 **Depth:** 3785.7' **Length:** 5.26 cm **Diameter:** 3.71 cm **Notes:** Brittle, broken piece
	**ETOF-4** **Well:** K. Lawson #1 **Depth:** 3790' **Length:** 5.33 cm **Diameter:** 3.77 cm **Notes:** Almost impermeable		**ETOF-5** **Well:** K. Lawson #1 **Depth:** 3803.7' **Length:** 5.48 cm **Diameter:** 3.69 cm **Notes:** Almost impermeable
	**ETOF-6** **Well:** K. Lawson #1 **Depth:** 3806.6' **Length:** 5.65 cm **Diameter:** 3.65 cm **Notes:** small fracture, higher permeability.		**ETOF-7** **Well:** K. Lawson #1 **Depth:** 3809.8' **Length:** 5.18 cm **Diameter:** 3.74 cm **Notes:** Much finer grains. Different material. Almost impermeable
	**ETOF-8** **Well:** **Depth:** 2791.8' **Length:** 7.47 cm **Diameter:** 3.82 cm **Notes:** Fred Wang's visit 11/08/11, higher permeability.		**ETOF-9** **Depth:** 3808' **Length:** 6.83 cm **Diameter:** 3.80 cm **Notes:** Fred Wang's visit 11/08/11, higher permeability.

Figure 31. Core photos and properties of ETOF core plugs.

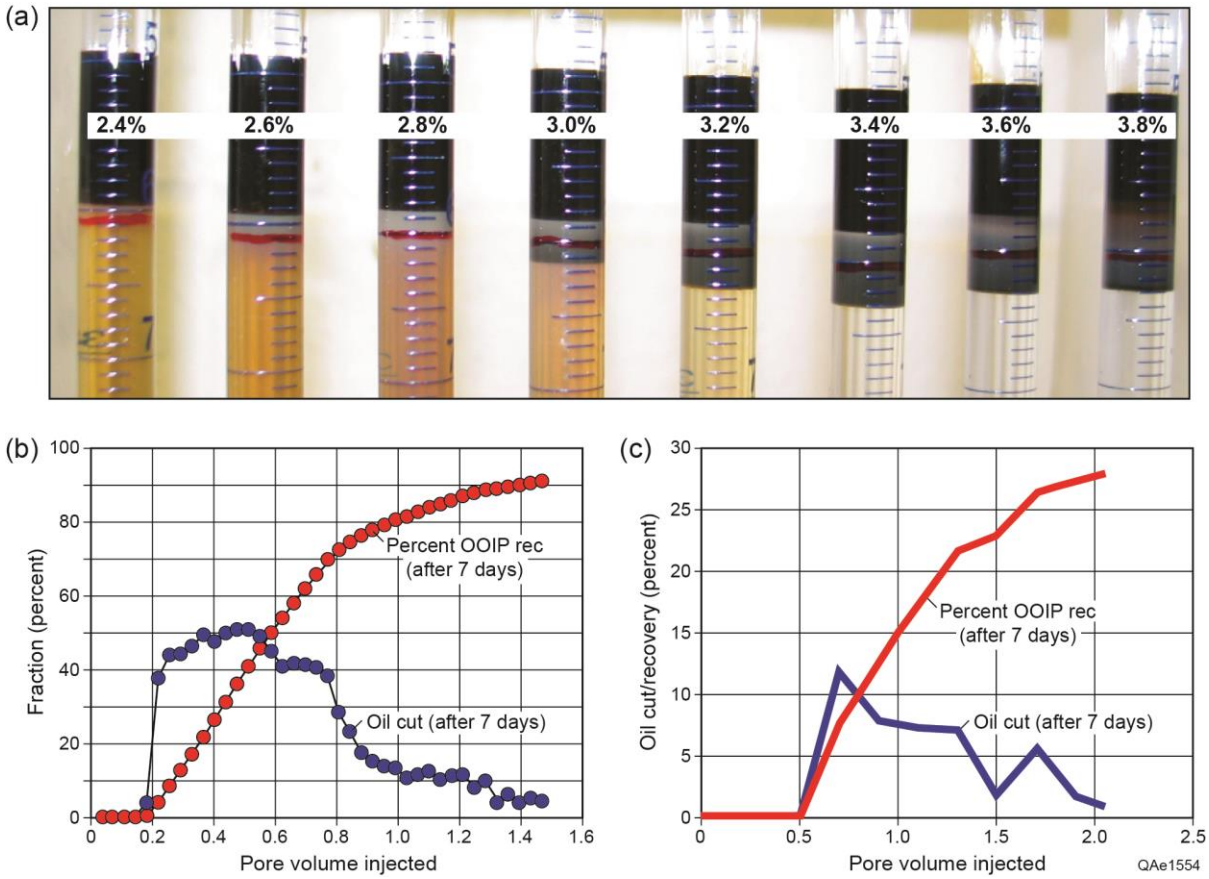

Figure 32. (a) Phase behavior of ASP composition used in coreflood, (b) cumulative oil recovery and oil cut of ASP flood using Berea Core #40 after equilibrating, and (c) oil cut and cumulative oil recovery of ASP flooding using ETOF Coreflood #4.

LIST OF ACRONYMS AND ABBREVIATIONS

Ac — acres

API — American Petroleum Institute

ASP — alkaline-surfactant polymer

BASA — business entity BASA Resources, Inc.

Bbl/d — barrels per day

BEG — Bureau of Economic Geology

BSTB — billion stock tank barrels

cc — cubic centimeter

Cp — centipoise, a unit of viscosity measurement

EOR — enhanced oil recovery

ETEA — East Texas Engineering Association

ETOF — East Texas Oil Field

EUR — estimated ultimate recovery

FS1…FS4 — stratigraphic terminology; designators for four Woodbine flooding surfaces

GIS — geographic information systems

GR — gamma-ray log

GU — gas unit

HCPV — hydrocarbon pore volume

K — permeability

LWB — Lower Woodbine (an abbreviation used in Hentz 2010)

Mbbl/day — thousand barrels per day

mD — millidarcies, a unit of permeability measurement

MFS — maximum flooding surface

MMSTB — million stock tank barrels

NPA — North Pilot Area

OOIP — original oil in place

(cont.)

PETRA — trade name for geological workstation software from IHS, Inc.

RF — recovery factor

ROIP — remaining oil in place

S1…S5 — stratigraphic terminology; designators for five Woodbine stratigraphic sequences

SB — sequence boundary

SCO2 — saturation of CO_2

SKU — South Kilgore Unit

SNF, Inc. — business entity, one of the world's leading manufacturers of water soluble polymers

Sor — oil saturation remaining

SorCO2 — oil saturation remaining after CO_2 flooding

SP — spontaneous potential log

SPA — South Pilot Area

STB — stock tank barrels

Swr — water saturation remaining

SwrCO2 — water saturation remaining after CO_2 flooding

TDA-12 — trade name for compound that includes toluenediamine (TDA)

TIPRO — Texas Independent Producers and Royalty Owners

TS — stratigraphic terminology: transgressive surface of erosion

TXOK — business entity TXOK Energy Resources Co.